J Math Chem (2010) 47:1420–1467
DOI 10.1007/s10910-010-9663-9

REVIEW PAPER

Review of theories on double electron capture in fast ion-atom collisions

Dževad Belkić

Received: 20 December 2009 / Accepted: 8 February 2010 / Published online: 11 March 2010

Abstract This work reviews quantum-mechanical four-body distorted wave theories for double electron capture in collisions between fast heavy multiply charged ions and heliumlike atomic systems. The widely used distorted wave methods of the first- and second-order in the pertinent perturbation series expansions are compared with each other. This tests the presumed importance of double continuum intermediate states of two electrons. Further, the relative performance is evaluated of the second-order theories with and without the eikonalization of the two-electron Coulomb wave functions for double continuum intermediate states. This checks the correctness and usefulness of the eikonalized Coulomb waves when two electrons participate actively to the transition from the initial to the final state of the entire system. We also analyze the significance of the contributions from excited heliumlike states especially in comparison between theory and measurement. The overall goal of the present study is to determine how much of the unprecedented experience gained over several decades in studying high-energy theories of pure three-body charge exchange could be exported directly to four-body double-electron capture without much of additional and essential eleaborations, besides the naturally increased computational demand. In particular, we address the unexpected breakdown of the continuum distorted wave eikonal initial state approximation and the anticipated success of continuum distorted wave theory for double charge exchange in ion-atom collisions at high impact energies.

Keywords Double-charge exchange · Two-electron transfer · High-energy atomic collisions · Leading distorted wave theories · Cross sections

Dž. Belkić (✉)
Karolinska Institute, P.O. Box 260, 171 76 Stockholm, Sweden
e-mail: Dzevad.Belkic@ki.se

1 Introduction

We review the existing quantum-mechanical four-body distorted wave theories for double electron capture in collisions between fast heavy multiply charged ions and heliumlike atomic systems [1–7]. The corresponding high-energy theories of pure three-body charge exchange have repeatedly been reviewed over the last several decades [8–14]. A strong emphasis has been given in the past to the eikonal initial states (EIS) [15–17]. These employ the well-known asymptotic phase factor of the single-electron Coulomb wave function in the entrance channel by which the well-established continuum distorted wave (CDW) method [8,18,19] is simplified to become the CDW-EIS approximation [15]. Here, the word "asymptote" refers to infinitely large distances between the electron and the nucleus in the field of which the continuum intermediate states are considered. The apparent success of this eikonalization cannot be explained on a sound theoretical basis, since merely empirical testings were used through comparisons with experimental data on charge exchange and ionization involving only one active electron. Normalization of the initial total scattering wave function was initially invoked as an attempt to theoretically justify the eikonalization [15,20]. However, this is not supported by consistency of theory, since the CDW-EIS approximation employs the unnormalized final states. If indeed the normalized scattering states were the main motivation for eikonalization, then the initial and final Coulomb wave functions for the continuum intermediate states ought to be treated on the same footing and, hence, both should be eikonalized. This was not done in purpose to avoid the ensuing degradation of the CDW-EIS approximation from the second- to the first-order perturbation modeling. Such a theoretically undesirable situation is the present motivation for a further assessment of the potential for systematics of the empirical success of the CDW-EIS approximation, but this time within a more stringent test on double charge exchange which occurs with a much weaker probability than one-electron transfer. An obvious *a priori* drawback of the CDW-EIS approximation is the loss of symmetry from the CDW approximation in treating the incident and target nuclear charge on the same footing. When one is willing to sacrifice this symmetry, then the possibility opens up for the introduction of other hybrid first- and second-order approximations with an alternative eikonalization of Coulomb continuum intermediate states, but this time for the relative motion of heavy nuclei. From the theoretical viewpoint, it is more justified to perform the eikonalization of Coulomb wave functions for inter-nuclear than for electron–nucleus interactions. This is exclusively due to the large reduced mass μ of two heavy nuclei. It is well-known that the replacement of the full Coulomb wave function for the inter-nuclear potential by its eikonal logarithmic phase factor gives the negligible $1/\mu^2$ contribution to the total cross section, even much below the Massey resonance peak and without the need to resort to any large, asymptotic distance. This sole theoretical argument suffices to anticipate that the hybrid second-order methods based upon the eikonalized Coulomb wave functions for the relative motion of heavy nuclei, such as the boundary-corrected continuum intermediate state (BCIS) [5] and the Born distorted wave (BDW) [21,22] methods, would exhibit similarly successful performance for single- and double-electron capture (as well as for multi-electron capture from multi-electron targets). This leads to yet another level of the present comprehensive testings by confronting the four-body versions of the CDW-EIS and BCIS

and BDW approximations for which their three-body variants are known to perform with a comparable success relative to measurements. Our choice of double capture is an excellent candidate for this type of testing aimed at determining which of the two mentioned eikonalizations for electronic or nuclear motions is more successful with respect to the corresponding experimental data.

Atomic units will be used throughout unless otherwise stated.

2 The CDW-4B method

We consider double electron capture:

$$Z_{\mathrm{P}} + (Z_{\mathrm{T}}; 2e)_i \longrightarrow (Z_{\mathrm{P}}, 2e)_f + Z_{\mathrm{T}}. \tag{2.1}$$

Here the parentheses symbolize bound states, whereas Z_{P} and Z_{T} are the charges of the projectile and target nucleus. The transition amplitude for double electron capture in the CDW-4B method becomes [7]:

$$\begin{aligned} T_{if}^{-} = -N^2 \iiint \mathrm{d}\boldsymbol{x}_1 \mathrm{d}\boldsymbol{x}_2 \mathrm{d}\boldsymbol{r}_i \, \mathrm{e}^{i\boldsymbol{k}_i\cdot\boldsymbol{r}_i + i\boldsymbol{k}_f\cdot\boldsymbol{r}_f} \mathcal{L}(\boldsymbol{r}_i, \boldsymbol{r}_f) \varphi_f^*(\boldsymbol{s}_1, \boldsymbol{s}_2) \\ \times {}_1F_1(i\nu_{\mathrm{T}}, 1, ivx_1 + i\boldsymbol{v}\cdot\boldsymbol{x}_1) \, {}_1F_1(i\nu_{\mathrm{T}}, 1, ivx_2 + i\boldsymbol{v}\cdot\boldsymbol{x}_2) \\ \times \Big\{ {}_1F_1(i\nu_{\mathrm{P}}, 1, ivs_2 + i\boldsymbol{v}\cdot\boldsymbol{s}_2) \nabla_{x_1}\varphi_i(\boldsymbol{x}_1, \boldsymbol{x}_2)\cdot\nabla_{s_1} \, {}_1F_1(i\nu_{\mathrm{P}}, 1, ivs_1 + i\boldsymbol{v}\cdot\boldsymbol{s}_1) \\ + \; {}_1F_1(i\nu_{\mathrm{P}}, 1, ivs_1 + i\boldsymbol{v}\cdot\boldsymbol{s}_1) \nabla_{x_2}\varphi_i(\boldsymbol{x}_1, \boldsymbol{x}_2)\cdot\nabla_{s_2} \, {}_1F_1(i\nu_{\mathrm{P}}, 1, ivs_2 + i\boldsymbol{v}\cdot\boldsymbol{s}_2) \Big\} \end{aligned} \tag{2.2}$$

with $N = N^+(\nu_{\mathrm{P}})N^+(\nu_{\mathrm{T}})$, $N^+(\nu_{\mathrm{K}}) = \Gamma(1 - i\nu_{\mathrm{K}})\mathrm{e}^{\pi\nu_{\mathrm{K}}/2}$, $\nu_{\mathrm{K}} = Z_{\mathrm{K}}/v \quad (\mathrm{K} = \mathrm{P}, \mathrm{T})$

$$\begin{aligned} \mathcal{L}(\boldsymbol{r}_i, \boldsymbol{r}_f) = \mu_i^{-2i\nu_{\mathrm{P}}} \mu_f^{-2i\nu_{\mathrm{T}}} [\mathcal{N}^-(\nu)]^2 \\ \times {}_1F_1(-i\nu, 1, ik_i r_f + i\boldsymbol{k}_i\cdot\boldsymbol{r}_f) \, {}_1F_1(-i\nu, 1, ik_f r_i + i\boldsymbol{k}_f\cdot\boldsymbol{r}_i), \end{aligned} \tag{2.3}$$

where $\mathcal{N}^{\pm}(\nu) = \Gamma(1 \mp i\nu)\mathrm{e}^{-\pi\nu/2}$ and $\nu = Z_{\mathrm{P}}Z_{\mathrm{T}}/v$. A simplification of (2.3) follows from the eikonal approximation:

$$\begin{aligned} &[\mathcal{N}^-(\nu)]^2 \, {}_1F_1(-i\nu, 1, ik_i r_f + i\boldsymbol{k}_i\cdot\boldsymbol{r}_f) \, {}_1F_1(-i\nu, 1, ik_f r_i + i\boldsymbol{k}_f\cdot\boldsymbol{r}_i) \\ &\simeq (k_i r_f + \boldsymbol{k}_i\cdot\boldsymbol{r}_f)^{i\nu} (k_f r_i + \boldsymbol{k}_f\cdot\boldsymbol{r}_i)^{i\nu} \simeq (\mu_i\mu_f)^{i\nu} [(vR - \boldsymbol{v}\cdot\boldsymbol{R})(vR + \boldsymbol{v}\cdot\boldsymbol{R})]^{i\nu} \\ &= (\mu_i\mu_f)^{i\nu} [v^2(R^2 - Z^2)]^{i\nu} = (\mu_i\mu_f)^{i\nu} (v\rho)^{2i\nu} \simeq (\mu v\rho)^{2i\nu} \\ &\therefore \qquad \mathcal{L}(\boldsymbol{r}_i, \boldsymbol{r}_f) \simeq \mu^{-2i(\nu_{\mathrm{P}} + \nu_{\mathrm{T}})} (\mu v\rho)^{2i\nu}, \end{aligned} \tag{2.4}$$

where $\mu = M_{\mathrm{P}}M_{\mathrm{T}}/(M_{\mathrm{P}} + M_{\mathrm{T}})$. Here, $\boldsymbol{\rho}$ is the projection of vector $\boldsymbol{R}$ to the XOY plane perpendicular to the Z-axis, i.e. $\boldsymbol{\rho} = \boldsymbol{R} - \boldsymbol{Z}$ with $\boldsymbol{\rho}\cdot\boldsymbol{Z} = 0$, where vector $\boldsymbol{Z}$ represents the projection of vector $\boldsymbol{R}$ to the Z-axis. The phase factor $(\mu v\rho)^{2i\nu}$, which

stems directly from the inter-nuclear potential $V_{\rm PT} = Z_{\rm P}Z_{\rm T}/R$, does not influence the total cross section, since:

$$Q_{if}^{-}\left(a_0^2\right) = \frac{1}{(2\pi v)^2}\int \mathrm{d}\boldsymbol{\eta}\left|T_{if}^{-}(\boldsymbol{\eta})\right|^2 = \int \mathrm{d}\boldsymbol{\eta}\left|\frac{R_{if}^{-}(\boldsymbol{\eta})}{2\pi v}\right|^2, \tag{2.5}$$

where

$$\begin{aligned} R_{if}^{-}(\boldsymbol{\eta}) = -N^2 \iiint \mathrm{d}\boldsymbol{x}_1\mathrm{d}\boldsymbol{x}_2\mathrm{d}\boldsymbol{r}_i\, \mathrm{e}^{i\boldsymbol{k}_i\cdot\boldsymbol{r}_i + i\boldsymbol{k}_f\cdot\boldsymbol{r}_f}\varphi_f^*(\boldsymbol{s}_1,\boldsymbol{s}_2) \\ \times {}_1F_1(i\nu_{\rm T},1,ivx_1 + i\boldsymbol{v}\cdot\boldsymbol{x}_1)\,{}_1F_1(i\nu_{\rm T},1,ivx_2 + i\boldsymbol{v}\cdot\boldsymbol{x}_2) \\ \times \Big\{ {}_1F_1(i\nu_{\rm P},1,ivs_2 + i\boldsymbol{v}\cdot\boldsymbol{s}_2)\nabla_{x_1}\varphi_i(\boldsymbol{x}_1,\boldsymbol{x}_2)\cdot\nabla_{s_1}\,{}_1F_1(i\nu_{\rm P},1,ivs_1 + i\boldsymbol{v}\cdot\boldsymbol{s}_1) \\ + {}_1F_1(i\nu_{\rm P},1,ivs_1 + i\boldsymbol{v}\cdot\boldsymbol{s}_1)\nabla_{x_2}\varphi_i(\boldsymbol{x}_1,\boldsymbol{x}_2)\cdot\nabla_{s_2}\,{}_1F_1(i\nu_{\rm P},1,ivs_2 + i\boldsymbol{v}\cdot\boldsymbol{s}_2)\Big\}. \end{aligned} \tag{2.6}$$

It is now obvious from (2.5) that the total cross section Q_{if}^{-} is independent of the inter-nuclear potential $Z_{\rm P}Z_{\rm T}/R$, as it should be [8]. The expression (2.6) for the basic matrix element R_{if}^{-} represents the main working expression for calculating the total cross sections. Such a CDW-4B method represents a strict generalization of Cheshire's CDW-3B method [18] for purely three-body single charge exchange:

$$Z_{\rm P} + (Z_{\rm T}, e)_i \longrightarrow (Z_{\rm P}, e)_f + Z_{\rm T}. \tag{2.7}$$

The result (2.6) for R_{if}^{-} in the CDW-4B method represents the rigorous first-order term in the four-body Dodd–Greider [23] perturbation series. This is very important, in view of the absence of any disconnected diagrams in the Dodd–Greider expansion, a feature which precludes divergence of the series. Only non-divergent perturbation series have a chance to provide the mathematically meaningful first-order terms that, in turn, could capture the major physical effects. Such is the CDW-4B method which can be called the four-body first-order continuum distorted wave (CDW-4B1) method. A similar remark also applies to the CDW-EIS-4B method which, therefore, can alternatively be termed the four-body first-order continuum distorted wave eikonal initial state (CDW-EIS-4B1) method.

The post form of the transition amplitude in the CDW-4B1 method reads as:

$$\begin{aligned} T_{if}^{+} = -N^2 \iiint \mathrm{d}\boldsymbol{s}_1\mathrm{d}\boldsymbol{s}_2\mathrm{d}\boldsymbol{r}_f\, \mathrm{e}^{i\boldsymbol{k}_i\cdot\boldsymbol{r}_i + i\boldsymbol{k}_f\cdot\boldsymbol{r}_f}\mathcal{L}(\boldsymbol{r}_i,\boldsymbol{r}_f)\varphi_i(\boldsymbol{x}_1,\boldsymbol{x}_2) \\ \times {}_1F_1(i\nu_{\rm P},1,ivs_1 + i\boldsymbol{v}\cdot\boldsymbol{s}_1)\,{}_1F_1(i\nu_{\rm P},1,ivs_2 + i\boldsymbol{v}\cdot\boldsymbol{s}_2) \\ \times \Big\{ {}_1F_1(i\nu_{\rm T},1,ivx_2 + i\boldsymbol{v}\cdot\boldsymbol{x}_2)\nabla_{s_1}\varphi_f^*(\boldsymbol{s}_1,\boldsymbol{s}_2)\cdot\nabla_{x_1}\,{}_1F_1(i\nu_{\rm T},1,ivx_1 + i\boldsymbol{v}\cdot\boldsymbol{x}_1) \\ + {}_1F_1(i\nu_{\rm T},1,ivx_1 + i\boldsymbol{v}\cdot\boldsymbol{x}_1)\nabla_{s_2}\varphi_f^*(\boldsymbol{s}_1,\boldsymbol{s}_2)\cdot\nabla_{x_2}\,{}_1F_1(i\nu_{\rm T},1,ivx_2 + i\boldsymbol{v}\cdot\boldsymbol{x}_2)\Big\}. \end{aligned} \tag{2.8}$$

The post total cross sections is:

$$Q_{if}^{+}\left(a_0^2\right)=\frac{1}{(2\pi v)^2}\int \mathrm{d}\boldsymbol{\eta}\left|T_{if}^{+}(\boldsymbol{\eta})\right|^2=\int \mathrm{d}\boldsymbol{\eta}\left|\frac{R_{if}^{+}(\boldsymbol{\eta})}{2\pi v}\right|^2, \tag{2.9}$$

where

$$\begin{aligned}R_{if}^{+}(\boldsymbol{\eta})=&-N^2\iiint \mathrm{d}\boldsymbol{s}_1\mathrm{d}\boldsymbol{s}_2\mathrm{d}\boldsymbol{r}_f\,\mathrm{e}^{i\boldsymbol{k}_i\cdot\boldsymbol{r}_i+i\boldsymbol{k}_f\cdot\boldsymbol{r}_f}\varphi_i(\boldsymbol{x}_1,\boldsymbol{x}_2)\\&\times {}_1F_1(i\nu_{\mathrm{P}},1,ivs_1+i\boldsymbol{v}\cdot\boldsymbol{s}_1)\,{}_1F_1(i\nu_{\mathrm{P}},1,ivs_2+i\boldsymbol{v}\cdot\boldsymbol{s}_2)\\&\times\Big\{{}_1F_1(i\nu_{\mathrm{T}},1,ivx_2+i\boldsymbol{v}\cdot\boldsymbol{x}_2)\nabla_{s_1}\varphi_f^{*}(\boldsymbol{s}_1,\boldsymbol{s}_2)\cdot\nabla_{x_1}{}_1F_1(i\nu_{\mathrm{T}},1,ivx_1+i\boldsymbol{v}\cdot\boldsymbol{x}_1)\\&+{}_1F_1(i\nu_{\mathrm{T}},1,ivx_1+i\boldsymbol{v}\cdot\boldsymbol{x}_1)\nabla_{s_2}\varphi_f^{*}(\boldsymbol{s}_1,\boldsymbol{s}_2)\cdot\nabla_{x_2}{}_1F_1(i\nu_{\mathrm{T}},1,ivx_2+i\boldsymbol{v}\cdot\boldsymbol{x}_2)\Big\}.\end{aligned} \tag{2.10}$$

The transition amplitude as a function of vector $\boldsymbol{\rho}$ can be obtained via:

$$a_{if}^{\pm}(\boldsymbol{\rho})=\frac{1}{2\pi v}\rho^{2i\nu}\int \mathrm{d}\boldsymbol{\eta}\,\mathrm{e}^{i\boldsymbol{\eta}\cdot\boldsymbol{\rho}}R_{if}^{\pm}(\boldsymbol{\eta}). \tag{2.11}$$

Using the Parseval relation, i.e. the convolution theorem for the Fourier integral in the total cross sections, we have:

$$Q_{if}^{\pm}\left(a_0^2\right)=\int \mathrm{d}\boldsymbol{\rho}\,|a_{if}^{\pm}(\boldsymbol{\rho})|^2. \tag{2.12}$$

The differential cross section in the CDW-3B and CDW-4B methods can be calculated directly from the expressions for $T_{if}^{\pm}$ [24,25]. Alternatively, we can first carry out the Fourier integral according to (2.11), and then use the following expression for the differential cross section [26–28]:

$$\frac{\mathrm{d}Q_{if}^{\pm}}{\mathrm{d}\Omega}=\left|i\mu v\int_0^{\infty}\mathrm{d}\rho\rho^{1+2i\nu}J_{m_i-m_f}\left(2\mu v\rho\sin\frac{\theta}{2}\right)a_{if}^{\pm}(\rho)\right|^2\left(\frac{a_0^2}{sr}\right), \tag{2.13}$$

where θ is the scattering angle in the center of mass frame of reference. Here, $J_\nu(z)$ is the Bessel function of the first order and the νth kind, whereas m_i and m_f are the magnetic quantum numbers of the initial and final bound state.

Calculation of the matrix elements for double electron capture into the ground state ($1s^2$) from any helium-like atom/ion has been carried out by Belkić and Mančev [7]. Their method of calculation provides the total cross section $Q_{if}^{\pm}$ through four-dimensional integrals that are subsequently computed by utilizing the scaled Gauss-Legendre and Gauss-Mehler quadratures [29–31]. It can be verified that in the symmetric resonant case ($i=f$, $Z_{\mathrm{P}}=Z_{\mathrm{T}}$), there is no post–prior discrepancy, i.e. $R_{if}^{-}=R_{if}^{+}$, so that $Q_{if}^{-}=Q_{if}^{+}$.

3 The SE-4B method

The CDW-4B method for double charge exchange treats two electrons and two nuclei in an entirely symmetric manner in the entrance and exit channel. In particular, the two-electron full Coulomb wave functions are used to describe double continuum intermediate states that distort the initial and final unperturbed states Φ_i and Φ_f. This double electronic distortion function is given by the product of two Coulomb wave functions (the so-called C2 wave function) centered either on the projectile or target nucleus in the entrance and exit channels. The behavior of each of the two Coulomb wave functions at large distances is given by the well-known asymptotes in terms of the logarithmic Coulomb phase factors. In particular, for $|vs_k + \boldsymbol{v}\cdot\boldsymbol{s}_k| \gg 1$ $(k = 1, 2)$, the leading asymptotic term in the product of the two confluent hyper-geometric functions from the C2 wave function is the twofold Coulomb logarithmic phase factor in the entrance channel:

$$\begin{aligned}[N^+(\nu_\mathrm{P})]^2\, {}_1F_1(i\nu_\mathrm{P}, 1, ivs_1 + i\boldsymbol{v}\cdot\boldsymbol{s}_1)\, {}_1F_1(i\nu_\mathrm{P}, 1, ivs_2 + i\boldsymbol{v}\cdot\boldsymbol{s}_2)\\ \approx (vs_1 + \boldsymbol{v}\cdot\boldsymbol{s}_1)^{-i\nu_\mathrm{P}}(vs_2 + \boldsymbol{v}\cdot\boldsymbol{s}_2)^{-i\nu_\mathrm{P}}.\end{aligned} \tag{3.1}$$

Likewise, in the exit channel we have for $|vx_k + \boldsymbol{v}\cdot\boldsymbol{x}_k| \gg 1$ $(k = 1, 2)$

$$\begin{aligned}[N^-(\nu_\mathrm{T})]^2\, {}_1F_1(-i\nu_\mathrm{T}, 1, -ivx_1 - i\boldsymbol{v}\cdot\boldsymbol{x}_1)\, {}_1F_1(-i\nu_\mathrm{T}, 1, -ivx_2 - i\boldsymbol{v}\cdot\boldsymbol{x}_2)\\ \approx (vx_1 + \boldsymbol{v}\cdot\boldsymbol{x}_1)^{i\nu_\mathrm{T}}(vx_2 + \boldsymbol{v}\cdot\boldsymbol{x}_2)^{i\nu_\mathrm{T}}.\end{aligned} \tag{3.2}$$

If one makes the additional approximations (3.1) and (3.2) to the exact CDW-4B method simultaneously in the entrance and exit channels, one obtains the four-body symmetric eikonal (SE-4B) method for double capture in process (2.1). The initial scattering state wave function in the SE-4B methods is:

$$\begin{aligned}\psi_i^+ = \mu_i^{-2i\nu_\mathrm{P}}\mathcal{N}^+(\nu)\mathrm{e}^{i\boldsymbol{k}_i\cdot\boldsymbol{r}_i}\, {}_1F_1(-i\nu, 1, ik_ir_f + i\boldsymbol{k}_i\cdot\boldsymbol{r}_f)\\ \times(vs_1 + \boldsymbol{v}\cdot\boldsymbol{s}_1)^{-i\nu_\mathrm{P}}(vs_2 + \boldsymbol{v}\cdot\boldsymbol{s}_2)^{-i\nu_\mathrm{P}}\end{aligned} \tag{3.3}$$

whereas the final state vector reads:

$$\begin{aligned}\psi_f^- = \mu_f^{2i\nu_\mathrm{T}}\mathcal{N}^-(\nu)\mathrm{e}^{-i\boldsymbol{k}_f\cdot\boldsymbol{r}_f}\, {}_1F_1(i\nu, 1, -ik_fr_i - i\boldsymbol{k}_f\cdot\boldsymbol{r}_i)\\ \times(vx_1 + \boldsymbol{v}\cdot\boldsymbol{x}_1)^{i\nu_\mathrm{T}}(vx_2 + \boldsymbol{v}\cdot\boldsymbol{x}_2)^{i\nu_\mathrm{T}}.\end{aligned} \tag{3.4}$$

Thus, the SE-4B method also treats both electrons on the same footing in the entrance and exit channels, as does the CDW-4B method, except that the former method uses the logarithmic phases instead of the original full Coulomb waves from the latter method. This modification of the electronic C2 wave function from the CDW-4B method must simultaneously be accompanied by the associated change in the perturbation interactions through the appearance of the two-electron kinetic energy operators alongside the usual gradient–gradient potential operators. These kinetic energy operators represent the additional perturbations introduced by eikonalization of the full

Coulomb wave functions. With these modifications, the prior form of the transition amplitude in the SE-4B method becomes:

$$
\begin{aligned}
T_{if}^{-} = -\iiint \mathrm{d}\boldsymbol{x}_1 \mathrm{d}\boldsymbol{x}_2 \mathrm{d}\boldsymbol{r}_i \, \mathrm{e}^{i\boldsymbol{k}_i\cdot\boldsymbol{r}_i + i\boldsymbol{k}_f\cdot\boldsymbol{r}_f} \mathcal{L}(\boldsymbol{r}_i, \boldsymbol{r}_f) \\
\times \varphi_f^*(\boldsymbol{s}_1, \boldsymbol{s}_2) \, (v x_1 + \boldsymbol{v}\cdot\boldsymbol{x}_1)^{-i\nu_\mathrm{T}} \, (v x_2 + \boldsymbol{v}\cdot\boldsymbol{x}_2)^{-i\nu_\mathrm{T}} \\
\times \left[\frac{1}{2}\nabla_{s_1}^2 + \frac{1}{2}\nabla_{s_2}^2 + \boldsymbol{\nabla}_{x_1}\varphi_i(\boldsymbol{x}_1, \boldsymbol{x}_2)\cdot\boldsymbol{\nabla}_{s_1} + \boldsymbol{\nabla}_{x_2}\varphi_i(\boldsymbol{x}_1, \boldsymbol{x}_2)\cdot\boldsymbol{\nabla}_{s_2} \right] \\
\times \varphi_i(\boldsymbol{x}_1, \boldsymbol{x}_2) \, (v s_1 + \boldsymbol{v}\cdot\boldsymbol{s}_1)^{-i\nu_\mathrm{P}} \, (v s_2 + \boldsymbol{v}\cdot\boldsymbol{s}_2)^{-i\nu_\mathrm{P}}. \qquad (3.5)
\end{aligned}
$$

Similarly, the post version of the T-matrix elements in the same method is:

$$
\begin{aligned}
T_{if}^{+} = -\iiint \mathrm{d}\boldsymbol{s}_1 \mathrm{d}\boldsymbol{s}_2 \mathrm{d}\boldsymbol{r}_f \, \mathrm{e}^{i\boldsymbol{k}_i\cdot\boldsymbol{r}_i + i\boldsymbol{k}_f\cdot\boldsymbol{r}_f} \mathcal{L}(\boldsymbol{r}_i, \boldsymbol{r}_f) \\
\times \varphi_i(\boldsymbol{x}_1, \boldsymbol{x}_2) \, (v s_1 + \boldsymbol{v}\cdot\boldsymbol{s}_1)^{-i\nu_\mathrm{P}} \, (v s_2 + \boldsymbol{v}\cdot\boldsymbol{s}_2)^{-i\nu_\mathrm{P}} \\
\times \left[\frac{1}{2}\nabla_{x_1}^2 + \frac{1}{2}\nabla_{x_2}^2 + \boldsymbol{\nabla}_{s_1}\varphi_f^*(\boldsymbol{s}_1, \boldsymbol{s}_2)\cdot\boldsymbol{\nabla}_{x_1} + \boldsymbol{\nabla}_{s_2}\varphi_f^*(\boldsymbol{s}_1, \boldsymbol{s}_2)\cdot\boldsymbol{\nabla}_{x_2} \right] \\
\times \varphi_f^*(\boldsymbol{s}_1, \boldsymbol{s}_2) \, (v x_1 + \boldsymbol{v}\cdot\boldsymbol{x}_1)^{-i\nu_\mathrm{T}} \, (v x_2 + \boldsymbol{v}\cdot\boldsymbol{x}_2)^{-i\nu_\mathrm{T}}. \qquad (3.6)
\end{aligned}
$$

Here, the function $\mathcal{L}(\boldsymbol{r}_i, \boldsymbol{r}_f)$ is taken from (2.3). In the consistent mass limit $M_{\mathrm{P,T}} \gg 1$, the eikonal form (2.4) can be used for $\mathcal{L}(\boldsymbol{r}_i, \boldsymbol{r}_f)$ omitting the unimportant phases of unit moduli, e.g. $(\mu v)^{2i\nu}\mu^{-2i(\nu_\mathrm{P}+\nu_\mathrm{T})}$. The remaining phase factor $\rho^{2i\nu}$, as the only contribution from the inter-nuclear potential $V_{\mathrm{PT}} = Z_\mathrm{P}Z_\mathrm{T}/R$, is important for differential cross sections $\mathrm{d}Q_{if}^{\mp}/\mathrm{d}\Omega$ computed by the Fourier–Bessel transform of the ρ-dependent transition amplitudes $a_{if}^{\mp}(\boldsymbol{\rho})$ via (2.11). The matrix elements $R_{if}^{\mp}(\boldsymbol{\eta})$ from (2.5) and (2.9) differ from $T_{if}^{\mp}$ in (3.5) and (3.6) only in the absence of the functions $\mathcal{L}(\boldsymbol{r}_i, \boldsymbol{r}_f)$. The inter-nuclear phase $\rho^{2i\nu}$ gives a significant contribution primarily at larger scattering angles. The phase factor $\rho^{2i\nu}$ disappears altogether from total cross sections $Q_{if}^{\mp}$ computed from (2.5), (2.9) or (2.12). This is expected, since the inter-nuclear potential cannot give any contribution to the total cross sections in the mass limits $M_{\mathrm{P,T}} \gg 1$ [8].

4 The CDW-EIS-4B method

The CDW-EIS-4B method is a hybrid asymmetrical model which treats the entrance and exit channels by the SE-4B and CDW-4B methods, respectively. Here, the two-electron eikonal initial state is employed, so that scattering wave function ψ_i^+ in the entrance channel is given by (3.3). The scattering wave function ψ_f^- in the final state for the exit channel is borrowed from the CDW-4B method. Therefore, the transition

amplitude in the CDW-EIS-4B method reads as:

$$
\begin{aligned}
T_{if}^{+} = -[N^{+}(\nu_{\mathrm{T}})]^{2} \iiint \mathrm{d}\boldsymbol{s}_1 \mathrm{d}\boldsymbol{s}_2 \mathrm{d}\boldsymbol{r}_f \, \mathrm{e}^{i\boldsymbol{k}_i\cdot\boldsymbol{r}_i + i\boldsymbol{k}_f\cdot\boldsymbol{r}_f} \mathcal{L}(\boldsymbol{r}_i, \boldsymbol{r}_f) \\
\times \varphi_i(\boldsymbol{x}_1, \boldsymbol{x}_2) \, (v s_1 + \boldsymbol{v}\cdot\boldsymbol{s}_1)^{-i\nu_{\mathrm{P}}} \, (v s_2 + \boldsymbol{v}\cdot\boldsymbol{s}_2)^{-i\nu_{\mathrm{P}}} \\
\times \Big\{ {}_1F_1(i\nu_{\mathrm{T}}, 1, ivx_2 + i\boldsymbol{v}\cdot\boldsymbol{x}_2) \nabla_{s_1} \varphi_f^{*}(\boldsymbol{s}_1, \boldsymbol{s}_2) \cdot \nabla_{x_1} {}_1F_1(i\nu_{\mathrm{T}}, 1, ivx_1 + i\boldsymbol{v}\cdot\boldsymbol{x}_1) \\
+ {}_1F_1(i\nu_{\mathrm{T}}, 1, ivx_1 + i\boldsymbol{v}\cdot\boldsymbol{x}_1) \nabla_{s_2} \varphi_f^{*}(\boldsymbol{s}_1, \boldsymbol{s}_2) \cdot \nabla_{x_2} {}_1F_1(i\nu_{\mathrm{T}}, 1, ivx_2 + i\boldsymbol{v}\cdot\boldsymbol{x}_2) \Big\} .
\end{aligned}
\tag{4.1}
$$

5 The CDW-EFS-4B method

The CDW-EFS-4B method is also a hybrid asymmetrical model, but here the entrance and exit channels are described by the CDW-4B and SE-4B methods, respectively. This time, the two-electron eikonal final state is used with the scattering wave function ψ_f^{-} in the exit channel given by (3.4). The scattering wave function ψ_i^{+} in the initial state for the entrance channel is taken from the CDW-4B method. Thus, the CDW-EFS-4B method is the mirror image of the CDW-EIS-4B method. The transition amplitude in the CDW-EFS-4B method is:

$$
\begin{aligned}
T_{if}^{-} = -[N^{+}(\nu_{\mathrm{P}})]^{2} \iiint \mathrm{d}\boldsymbol{x}_1 \mathrm{d}\boldsymbol{x}_2 \mathrm{d}\boldsymbol{r}_i \, \mathrm{e}^{i\boldsymbol{k}_i\cdot\boldsymbol{r}_i + i\boldsymbol{k}_f\cdot\boldsymbol{r}_f} \mathcal{L}(\boldsymbol{r}_i, \boldsymbol{r}_f) \\
\times \varphi_f^{*}(\boldsymbol{s}_1, \boldsymbol{s}_2) \, (v x_1 + \boldsymbol{v}\cdot\boldsymbol{x}_1)^{-i\nu_{\mathrm{T}}} \, (v x_2 + \boldsymbol{v}\cdot\boldsymbol{x}_2)^{-i\nu_{\mathrm{T}}} \\
\times \Big\{ {}_1F_1(i\nu_{\mathrm{P}}, 1, ivs_2 + i\boldsymbol{v}\cdot\boldsymbol{s}_2) \nabla_{x_1} \varphi_i(\boldsymbol{x}_1, \boldsymbol{x}_2) \cdot \nabla_{s_1} {}_1F_1(i\nu_{\mathrm{P}}, 1, ivs_1 + i\boldsymbol{v}\cdot\boldsymbol{s}_1) \\
+ {}_1F_1(i\nu_{\mathrm{P}}, 1, ivs_1 + i\boldsymbol{v}\cdot\boldsymbol{s}_1) \nabla_{x_2} \varphi_i(\boldsymbol{x}_1, \boldsymbol{x}_2) \cdot \nabla_{s_2} {}_1F_1(i\nu_{\mathrm{P}}, 1, ivs_2 + i\boldsymbol{v}\cdot\boldsymbol{s}_2) \Big\} .
\end{aligned}
\tag{5.1}
$$

Regarding differential as well as total cross sections, the same procedure from the CDW-4B or SE-4B methods also applies to the CDW-EIS-4B and CDW-EFS-4B methods. This amounts to using the generic expressions (2.11), (2.5), (2.9) and (2.12). In these latter formulae, the matrix elements $R_{if}^{+}(\boldsymbol{\eta})$ and $R_{if}^{-}(\boldsymbol{\eta})$ coincide with the transition amplitudes T_{if}^{+} and T_{if}^{-} from (4.1) and (5.1) provided that the function $\mathcal{L}(\boldsymbol{r}_i, \boldsymbol{r}_f)$ from (2.4) due to the inter-nuclear distortion is set to unity, as justified by $M_{\mathrm{P,T}} \gg 1$.

We reiterate that the CDW-EIS-4B and CDW-EFS-4B methods are two different approximate variants to the CDW-4B method. The supplementary approximations consist of replacing the electronic C2 wave functions from the CDW-4B method by their asymptotic forms (Coulomb logarithmic phase factors) in one of the two channels (the entrance or exit channel in the CDW-EIS-4B or CDW-EFS-4B methods, respectively). However, these further approximations introduced by the CDW-EIS-4B and CDW-EFS-4B methods destroy the original symmetric treatments of two electrons and two nuclei in the CDW-4B method.

The above setting of the SE-4B (prior, post), CDW-EIS-4B and CDW-EFS-4B methods stems simply from making further approximations (of varying severity) to the already available expressions from the exact CDW-4B method. Such a setting directly establishes the connections among different methods. The found relationships facilitate comparisons among these methods, so that potentially notable differences in the obtained results could be interpreted in terms of the corresponding degrees of physical mechanisms invoked in different approximations. Alternatively, one can derive the SE-4B, CDW-EIS-4B and CDW-EFS-4B methods without recourse to the CDW-4B method by making separate choices of distorting potentials and subsequently solving the resulting equations for the distorted waves. Such an analysis within the SE-4B, CDW-EIS-4B and CDW-EFS-4B methods might give the wrong impression that these approximations are unrelated to the CDW-4B method. However, irrespective of the way in which the derivation proceeds, one inevitably obtains the same results as given in the above succinct outlines (with no derivation whatsoever) by appropriately approximating the CDW-4B method. Hence the needed relationship.

The important question to ask is: why should one make the eikonal approximations to the electronic distorting functions in the initial or final states if these latter functions could be treated exactly? Do the supplementary approximations eventually simplify the computations by a sizeable factor? And, most importantly, is there any significant physical effect which is lost by these eikonalizations?

For three-body problems, the SE-3B method gives closed analytical expressions for single charge exchange, relative to the corresponding one-dimensional numerical quadrature in the CDW-3B method. Nevertheless, the difference in the computational effort invested to generate the needed tables and data bases for cross sections is negligible, since a single numerical integration is a trivial task by any standard. However, the SE-3B method irretrievably loses the important Thomas double scattering mechanism [32], which on the other hand is described by the CDW-3B method. This is manifested by the BK1-3B type $\propto v^{-12-2l_i-2l_f}$-behavior of $Q_{if}^{(\mathrm{SE-3B})}$ in the limit of high impact velocities v for fixed values of the angular momenta l_i and l_f in the initial and final bound-state hydrogen-like wave functions. By contrast, the CDW-3B method and experiments give a completely different second Born type v^{-11}-behavior for arbitrary values of l_i and l_f. In the case of the SE-4B method for double capture, no analytical results can be obtained for the transition amplitude, let alone cross sections. In other words, computational efforts are again comparable in the SE-4B and CDW-4B methods. As to the billiard-type scattering mechanisms of Thomas [32], the situation becomes even more aggravated with eikonalization of the full twofold electronic continua, since double capture is expected to exhibit three Thomas peaks [21,22] and none of them can be predicted by the SE-4B method.

Since the CDW-EIS-3B or CDW-EFS-3B methods use the eikonal continuum intermediate states in the entrance or exit channel, it is anticipated that these two approximations will preserve the mentioned unphysical features of the SE-3B method. By the same token, the CDW-EIS-3B or CDW-EFS-3B methods will inherit the good features of the CDW-3B method in the relevant parts concerned with the complementary exit or entrance channels, respectively. This can be seen in the corresponding high-velocity asymptotic formulae of the total cross sections $Q_{if}^{(\mathrm{CDW-EIS-3B})} \propto v^{-11-2l_i}$

(any l_f) and $Q_{if}^{(\mathrm{CDW-EFS-3B})} \propto v^{-11-2l_f}$ (any l_i) instead of the correct asymptote $Q_{if}^{(\mathrm{CDW-3B})} \propto v^{-11}$ (any l_i and l_f). Analogous and possibly more severe failures could occur by passing to four-body problems such as double capture when studied by means of the CDW-EIS-4B and CDW-EFS-4B methods. This will be analyzed in the section with illustrations for two-electron transfer in process (2.1).

6 The BDW-4B method

The CDW-4B method takes full account of the double Coulomb wave functions due to the potentials $V_{\mathrm{P}_k} = -Z_\mathrm{P}/s_k$ and $V_{\mathrm{T}_k} = -Z_\mathrm{T}/x_k$ ($k = 1, 2$) for describing the continuum intermediate states of the two electrons e_1 and e_2 at all distances s_k and x_k (finite, in the interaction region, and infinitely large, in the asymptotic region) in the entrance and exit channel, respectively.

On the other hand, in the boundary-corrected first Born (CB1-4B) method, the motions for the same two electrons are distorted in a much simpler way by including only the twofold Coulomb logarithmic phases due to the electrons-nuclei potentials in the initial and final asymptotic regions $V_\mathrm{P}^\infty = -2Z_\mathrm{P}/R$ and $V_\mathrm{T}^\infty = -2Z_\mathrm{T}/R$, respectively. The potentials $V_{\mathrm{P}_1} + V_{\mathrm{P}_2}$ and $V_{\mathrm{T}_1} + V_{\mathrm{T}_2}$ tend to V_P^∞ and V_T^∞, since in the initial and final asymptotic regions, where $s_k \longrightarrow \infty$ and $x_k \longrightarrow \infty$, we have $s_k \approx R$ and $x_k \approx R$ (for both $k = 1$ and $k = 2$) in the entrance and exit channel, respectively. As a result, the corresponding continua are included through the electron asymptotic distortion phase factors $\exp[-2\nu_\mathrm{P} \ln(vR - \boldsymbol{v}\cdot\boldsymbol{R})]$ and $\exp[2\nu_\mathrm{T} \ln(vR + \boldsymbol{v}\cdot\boldsymbol{R})]$ due to V_P^∞ and V_T^∞, where $\nu_\mathrm{K} = Z_\mathrm{K}/v$ (K = P, T). Such phases remain in the computation for both differential and total cross sections in the CB1-4B method. Despite the explicit appearance of the vector $\boldsymbol{R}$, which happens to be the vector of the inter-nuclear distance, these electron asymptotic phases have nothing to do with the inter-nuclear repulsive potential itself, which is $V_\mathrm{PT} = Z_\mathrm{P}Z_\mathrm{T}/R$. The potential V_PT distorts the relative motion of the two nuclei P and T in both scattering channels, thus leading to the product of the associated asymptotic initial and final phases, $\exp[i\nu \ln(vR - \boldsymbol{v}\cdot\boldsymbol{R})]$ and $\{\exp[-\nu \ln(vR + \boldsymbol{v}\cdot\boldsymbol{R})]\}^*$ in the transition amplitude, where $\nu = Z_\mathrm{P}Z_\mathrm{T}/v$. The said product, which is equal to $(v\rho)^{2i\nu}$, is the only effect caused by the presence of V_PT in the exact eikonal four-body transition amplitude. With such an occurrence, it is easily shown that the ensuing exact eikonal total cross section is independent of $(v\rho)^{2i\nu}$ and, hence, of the inter-nuclear potential V_PT, as it ought to be on physical grounds [8]. Of course, this remains true for every particular approximation, provided that the correct boundary conditions are satisfied.

When in the entrance channel, the electronic and nuclear asymptotic Coulomb phase factors $\exp[-2\nu_P \ln(vR - \boldsymbol{v}\cdot\boldsymbol{R})]$ and $\exp[i\nu \ln(vR - \boldsymbol{v}\cdot\boldsymbol{R})]$ are added together, the total phase follows via $\exp[i\nu_i \ln(vR - \boldsymbol{v}\cdot\boldsymbol{R})]$, where $\nu_i = Z_\mathrm{P}(Z_\mathrm{T} - 2)/v$. This latter composite phase indicates that, on the level of determining the distortion of the unperturbed state Φ_i in the entrance channel, the presence of the two electrons is felt, in effect, merely through a screening of Z_T to yield the effective nuclear charge $Z_\mathrm{T} - 2$. The deduced $\boldsymbol{R}$-dependent total distortion phase factor is now recognized as being due to the asymptotic value $V_f^\infty = Z_\mathrm{T}(Z_\mathrm{P} - 2)/R$ of the perturbation V_f in the entrance channel. Similarly in the exit channel, the electron and nuclear asymptotic phase

factors $\exp[2\nu_P \ln(vR + \boldsymbol{v}\cdot\boldsymbol{R})]$ and $\exp[-i\nu \ln(vR + \boldsymbol{v}\cdot\boldsymbol{R})]$ yield the overall distortion $\exp[-i\nu_f \ln(vR + \boldsymbol{v}\cdot\boldsymbol{R})]$, where $\nu_f = Z_T(Z_P - 2)/v$. Here, the combined phase shows that the sole role for the electron distortion is to screen Z_P to $Z_P - 2$. Hence, such a reasoning on the level of the total $\boldsymbol{R}$-dependent distortion phase factor recovers the form of the asymptotic value $V_f^{\infty} = Z_T(Z_P - 2)/R$ of the perturbation V_f in the entrance channel.

Double ionization dominates over double charge exchange at high energies. Therefore, to properly describe electron transfer to a final bound state, in the limit of high energies, the electronic continuum intermediate states should be included at all distances, and this is fully accomplished in the CDW-4B method. Conversely, at lower energies, two-electron transfer dominates over ionization. This time, the electronic continuum states represent a drawback, since they overweigh the intermediate ionization paths of the studied reaction. Consequently, the CDW-4B method for double capture overestimates the corresponding experimental data at lower energies, as is also the case with single capture within the CDW-3B method [33–53].

The models that partially mitigate the over-account of continuum intermediate states at lower energies are certain hybrid approximations that combine the CDW-4B method in one channel with the CB1-4B method in the other channel. An example from this hybrid category is the BDW-4B method of Belkić [21]. Specifically, the BDW-4B method exactly coincides with the CDW-4B method in one channel and with the CB1-4B method in the other channel. As such, the BDW-4B method preserves the correct boundary conditions in both scattering channels, since both the CDW-4B and CB1-4B methods do so.

The transition amplitude in the prior form of the BDW-4B method is:

$$
\begin{aligned}
T_{if}^{(\mathrm{BDW})-} = -N_P \iiint \mathrm{d}\boldsymbol{x}_1 \mathrm{d}\boldsymbol{x}_2 \mathrm{d}\boldsymbol{r}_i \, \mathrm{e}^{i\boldsymbol{k}_i\cdot\boldsymbol{r}_i + i\boldsymbol{k}_f\cdot\boldsymbol{r}_f} \mathcal{L}_1(\boldsymbol{r}_i, \boldsymbol{r}_f)\varphi_f^*(\boldsymbol{s}_1, \boldsymbol{s}_2) \\
\times \Big\{ {}_1F_1(i\nu_P, 1, ivs_2 + i\boldsymbol{v}\cdot\boldsymbol{s}_2)\nabla_{x_1}\varphi_i(\boldsymbol{x}_1, \boldsymbol{x}_2)\cdot\nabla_{s_1} {}_1F_1(i\nu_P, 1, ivs_1 + i\boldsymbol{v}\cdot\boldsymbol{s}_1) \\
+ {}_1F_1(i\nu_P, 1, ivs_1 + i\boldsymbol{v}\cdot\boldsymbol{s}_1)\nabla_{x_2}\varphi_i(\boldsymbol{x}_1, \boldsymbol{x}_2)\cdot\nabla_{s_2} {}_1F_1(i\nu_P, 1, ivs_2 + i\boldsymbol{v}\cdot\boldsymbol{s}_2) \Big\}
\end{aligned}
\tag{6.1}
$$

where $N_P = [N^+(\nu_P)]^2$ and $\nu_P = Z_P/v$. Here, we have:

$$
\begin{aligned}
\mathcal{L}_1(\boldsymbol{r}_i, \boldsymbol{r}_f) = \frac{\mathcal{N}_1}{\mu_i^{2i\nu_P}} {}_1F_1(-i\nu, 1, ik_i r_f + i\boldsymbol{k}_i\cdot\boldsymbol{r}_f) \\
\times {}_1F_1(-i\nu_f, 1, ik_f r_i + i\boldsymbol{k}_f\cdot\boldsymbol{r}_i)
\end{aligned}
\tag{6.2}
$$

where $\mathcal{N}_1 = \mathcal{N}^+(\nu)\mathcal{N}^{-*}(\nu_f)$. Within the eikonal approximation, the following simplification is possible:

$$
\begin{aligned}
\mathcal{L}_1(\boldsymbol{r}_i, \boldsymbol{r}_f) &\simeq \mu_i^{i\nu_i}\mu_f^{i\nu_f} \mathrm{e}^{i\nu_f \ln(vR+\boldsymbol{v}\cdot\boldsymbol{R})} \mathrm{e}^{i\nu \ln(vR-\boldsymbol{v}\cdot\boldsymbol{R})} \\
&\simeq \mu^{-i(\xi_P+\xi_T)}(\mu v\rho)^{2i\nu} \mathrm{e}^{-i\xi_T \ln(vR+\boldsymbol{v}\cdot\boldsymbol{R})},
\end{aligned}
\tag{6.3}
$$

where

$$\nu_i = \frac{Z_{\rm P}(Z_{\rm T}-2)}{v}, \quad \nu_f = \frac{Z_{\rm T}(Z_{\rm P}-2)}{v}, \quad \xi_{\rm K} = 2\nu_{\rm K} = 2\frac{Z_{\rm K}}{v} \quad ({\rm K} = {\rm P}, {\rm T}). \tag{6.4}$$

Then, the total cross section can be found from (2.5), with R_{if}^{-} replaced by $R_{if}^{({\rm BDW})-}$, where:

$$\begin{aligned} R_{if}^{({\rm BDW})-}(\boldsymbol{\eta}) = -N_{\rm P} \iiint {\rm d}\boldsymbol{x}_1 {\rm d}\boldsymbol{x}_2 {\rm d}\boldsymbol{R}\, {\rm e}^{i\boldsymbol{k}_i\cdot\boldsymbol{r}_i + i\boldsymbol{k}_f\cdot\boldsymbol{r}_f} \\ \times \varphi_f^*(\boldsymbol{s}_1, \boldsymbol{s}_2)(vR + \boldsymbol{v}\cdot\boldsymbol{R})^{-i\xi_{\rm T}} \\ \times \Big\{ {}_1F_1(i\nu_{\rm P}, 1, ivs_2 + i\boldsymbol{v}\cdot\boldsymbol{s}_2)\nabla_{x_1}\varphi_i(\boldsymbol{x}_1, \boldsymbol{x}_2)\cdot\nabla_{s_1} {}_1F_1(i\nu_{\rm P}, 1, ivs_1 + i\boldsymbol{v}\cdot\boldsymbol{s}_1) \\ + {}_1F_1(i\nu_{\rm P}, 1, ivs_1 + i\boldsymbol{v}\cdot\boldsymbol{s}_1)\nabla_{x_2}\varphi_i(\boldsymbol{x}_1, \boldsymbol{x}_2)\cdot\nabla_{s_2} {}_1F_1(i\nu_{\rm P}, 1, ivs_2 + i\boldsymbol{v}\cdot\boldsymbol{s}_2)\Big\}. \end{aligned} \tag{6.5}$$

The corresponding post form of the transition amplitude is:

$$\begin{aligned} T_{if}^{({\rm BDW})+} = -N_{\rm T} \iiint {\rm d}\boldsymbol{s}_1 {\rm d}\boldsymbol{s}_2 {\rm d}\boldsymbol{r}_f {\rm e}^{i\boldsymbol{k}_i\cdot\boldsymbol{r}_i + i\boldsymbol{k}_f\cdot\boldsymbol{r}_f} \mathcal{L}_2(\boldsymbol{r}_i, \boldsymbol{r}_f)\varphi_i(\boldsymbol{x}_1, \boldsymbol{x}_2) \\ \times \Big\{ {}_1F_1(i\nu_{\rm T}, 1, ivx_2 + i\boldsymbol{v}\cdot\boldsymbol{x}_2)\nabla_{s_1}\varphi_f^*(\boldsymbol{s}_1, \boldsymbol{s}_2)\cdot\nabla_{x_1} {}_1F_1(i\nu_{\rm T}, 1, ivx_1 + i\boldsymbol{v}\cdot\boldsymbol{x}_1) \\ + {}_1F_1(i\nu_{\rm T}, 1, ivx_1 + i\boldsymbol{v}\cdot\boldsymbol{x}_1)\nabla_{s_2}\varphi_f^*(\boldsymbol{s}_1, \boldsymbol{s}_2)\cdot\nabla_{x_2} {}_1F_1(i\nu_{\rm T}, 1, ivx_2 + i\boldsymbol{v}\cdot\boldsymbol{x}_2)\Big\} \end{aligned} \tag{6.6}$$

where

$$\begin{aligned} \mathcal{L}_2(\boldsymbol{r}_i, \boldsymbol{r}_f) = \frac{\mathcal{N}_2}{\mu_f^{2i\nu_{\rm T}}} {}_1F_1(-i\nu_i, 1, ik_i r_f + i\boldsymbol{k}_i\cdot\boldsymbol{r}_f) \\ \times {}_1F_1(-i\nu, 1, ik_f r_i + i\boldsymbol{k}_f\cdot\boldsymbol{r}_i), \end{aligned} \tag{6.7}$$

with $N_{\rm T} = [N^{-*}(\nu_{\rm T})]^2$, $\mathcal{N}_2 = \mathcal{N}^+(\nu_i)\mathcal{N}^{-*}(\nu)$ and $\nu = Z_{\rm P}Z_{\rm T}/v$. The function $\mathcal{L}_2(\boldsymbol{r}_i, \boldsymbol{r}_f)$ can also be expressed in the eikonal approximation via:

$$\begin{aligned} \mathcal{L}_2(\boldsymbol{r}_i, \boldsymbol{r}_f) &\simeq \mu_i^{i\nu_i}\mu_f^{i\nu_f} {\rm e}^{i\nu_i \ln(vR - \boldsymbol{v}\cdot\boldsymbol{R})} {\rm e}^{i\nu \ln(vR + \boldsymbol{v}\cdot\boldsymbol{R})} \\ &\simeq \mu^{-i(\xi_{\rm P} + \xi_{\rm T})}(\mu v\rho)^{2i\nu} {\rm e}^{-i\xi_{\rm P} \ln(vR - \boldsymbol{v}\cdot\boldsymbol{R})}. \end{aligned} \tag{6.8}$$

Therefore, the total cross section is given by:

$$Q_{if}^{({\rm BDW})\pm}\left(a_0^2\right) = \int {\rm d}\boldsymbol{\eta} \left| \frac{R_{if}^{({\rm BDW})\pm}(\boldsymbol{\eta})}{2\pi v} \right|^2, \tag{6.9}$$

where

$$R_{if}^{(\mathrm{BDW})+}(\boldsymbol{\eta}) = -N_{\mathrm{T}} \iiint \mathrm{d}\boldsymbol{s}_1 \mathrm{d}\boldsymbol{s}_2 \mathrm{d}\boldsymbol{R}\, \mathrm{e}^{i\boldsymbol{k}_i\cdot\boldsymbol{r}_i + i\boldsymbol{k}_f\cdot\boldsymbol{r}_f} \times \varphi_i(\boldsymbol{x}_1, \boldsymbol{x}_2)(vR - \boldsymbol{v}\cdot\boldsymbol{R})^{-i\xi_{\mathrm{P}}} \times \Big\{ {}_1F_1(i\nu_{\mathrm{T}}, 1, ivx_2 + i\boldsymbol{v}\cdot\boldsymbol{x}_2) \nabla_{s_1}\varphi_f^*(\boldsymbol{s}_1, \boldsymbol{s}_2)\cdot\nabla_{x_1}\, {}_1F_1(i\nu_{\mathrm{T}}, 1, ivx_1 + i\boldsymbol{v}\cdot\boldsymbol{x}_1) + {}_1F_1(i\nu_{\mathrm{T}}, 1, ivx_1 + i\boldsymbol{v}\cdot\boldsymbol{x}_1) \nabla_{s_2}\varphi_f^*(\boldsymbol{s}_1, \boldsymbol{s}_2)\cdot\nabla_{x_2}\, {}_1F_1(i\nu_{\mathrm{T}}, 1, ivx_2 + i\boldsymbol{v}\cdot\boldsymbol{x}_2) \Big\}. \tag{6.10}$$

Notice that $R_{if}^{(\mathrm{BDW})-}$ can be obtained directly from $R_{fi}^{(\mathrm{BDW})+}$ by making the transformations $\boldsymbol{s}_1 \longleftrightarrow \boldsymbol{s}_2$ and $\boldsymbol{x}_1 \longleftrightarrow \boldsymbol{x}_2$ in both (6.5) and (6.10). This is possible because the vector $\boldsymbol{R}$ is invariant under this latter transformation. In such a case, these transformations will map the first of the two terms in $R_{if}^{(\mathrm{BDW})\pm}$ into the second term and vice versa. In other words, the contributions to $R_{if}^{(\mathrm{BDW})\pm}$ coming from $\boldsymbol{\nabla}_1\cdot\boldsymbol{\nabla}_1$ and $\boldsymbol{\nabla}_2\cdot\boldsymbol{\nabla}_2$ are identical to each other. Hence, these expressions can be rewritten as follows:

$$R_{if}^{(\mathrm{BDW})-}(\boldsymbol{\eta}) = -2N_{\mathrm{P}} \iiint \mathrm{d}\boldsymbol{x}_1 \mathrm{d}\boldsymbol{x}_2 \mathrm{d}\boldsymbol{R}\, \mathrm{e}^{i\boldsymbol{k}_i\cdot\boldsymbol{r}_i + i\boldsymbol{k}_f\cdot\boldsymbol{r}_f} \times (vR + \boldsymbol{v}\cdot\boldsymbol{R})^{-i\xi_{\mathrm{T}}} \varphi_f^*(\boldsymbol{s}_1, \boldsymbol{s}_2)\, F_{\mathrm{P}}(\boldsymbol{x}_1, \boldsymbol{x}_2; \boldsymbol{s}_1, \boldsymbol{s}_2) \tag{6.11}$$

and

$$R_{if}^{(\mathrm{BDW})+}(\boldsymbol{\eta}) = -2N_{\mathrm{T}} \iiint \mathrm{d}\boldsymbol{s}_1 \mathrm{d}\boldsymbol{s}_2 \mathrm{d}\boldsymbol{R}\, \mathrm{e}^{i\boldsymbol{k}_i\cdot\boldsymbol{r}_i + i\boldsymbol{k}_f\cdot\boldsymbol{r}_f} \times (vR - \boldsymbol{v}\cdot\boldsymbol{R})^{-i\xi_{\mathrm{P}}} \varphi_i(\boldsymbol{x}_1, \boldsymbol{x}_2)\, F_{\mathrm{T}}(\boldsymbol{x}_1, \boldsymbol{x}_2; \boldsymbol{s}_1, \boldsymbol{s}_2) \tag{6.12}$$

where

$$F_{\mathrm{P}}(\boldsymbol{x}_1, \boldsymbol{x}_2; \boldsymbol{s}_1, \boldsymbol{s}_2) = {}_1F_1(i\nu_{\mathrm{P}}, 1, ivs_2 + i\boldsymbol{v}\cdot\boldsymbol{s}_2) \times \nabla_{x_1}\varphi_i(\boldsymbol{x}_1, \boldsymbol{x}_2)\cdot\nabla_{s_1}\, {}_1F_1(i\nu_{\mathrm{P}}, 1, ivs_1 + i\boldsymbol{v}\cdot\boldsymbol{s}_1) \tag{6.13}$$

$$F_{\mathrm{T}}(\boldsymbol{x}_1, \boldsymbol{x}_2; \boldsymbol{s}_1, \boldsymbol{s}_2) = {}_1F_1(i\nu_{\mathrm{T}}, 1, ivx_2 + i\boldsymbol{v}\cdot\boldsymbol{x}_2) \times \nabla_{s_1}\varphi_f^*(\boldsymbol{s}_1, \boldsymbol{s}_2)\cdot\nabla_{x_1}\, {}_1F_1(i\nu_{\mathrm{T}}, 1, ivx_1 + i\boldsymbol{v}\cdot\boldsymbol{x}_1). \tag{6.14}$$

The physical interpretation of the prior form of the T-matrix element in the BDW-4B method can be done in the following plausible manner. The incident particle scatters on each of the three constituents of the target $(Z_{\mathrm{T}}; e_1, e_2)$. In the entrance channel, collision between the projectile Z_{P} and target nucleus Z_{T} results in accumulation of the Coulombic phase factor $\exp[(i/v)Z_{\mathrm{P}}Z_{\mathrm{T}}\ln(vR - \boldsymbol{v}\cdot\boldsymbol{R})]$. On the other hand, in the exit channel, the target nucleus Z_{T} interacts with the newly formed atom or ion $(Z_{\mathrm{P}}, 2e)_f$ considered as the point charge $(Z_{\mathrm{P}} - 2)$, thus accumulating the phase factor $\exp[-(i/v)Z_{\mathrm{T}}(Z_{\mathrm{P}} - 2)\ln(vR + \boldsymbol{v}\cdot\boldsymbol{R})]$ due to the asymptotic residual Coulombic interaction $W_f = Z_{\mathrm{T}}(Z_{\mathrm{P}} - 2)/R = V_f^{\infty}$. Thus, the nucleus T sees the two electrons

as playing the role of screening the nuclear charge Z_P to its effective value $Z_P - 2$ in the helium-like atomic system $(Z_P, 2e)_f$. In contrast, in the entrance channel, the BDW-4B method allows the projectile to separately distort the nuclear and electronic motions through the additive three Coulombic interactions. Thus, the interaction of Z_P with the electrons e_1 and e_2 leads to double ionization of the target $(Z_T; e_1, e_2)_i$. The ionized electrons propagate in the Coulomb field of Z_P in a particular eikonal direction with the momenta $\boldsymbol{\kappa}_1 \approx \boldsymbol{\kappa}_2 \approx \boldsymbol{v}$. Finally, capture of the two electrons occurs from these intermediate ionizing states (capture from continuum), because these electrons are traveling along each other, as well as together with the projectile in the same direction, such that the attractive potential between Z_P and e_k $(k = 1, 2)$ is sufficient to bind them together into the new helium-like atomic system $(Z_P; e_1, e_2)_f$. This is a quantum version of the well-known Thomas [32] classical double scattering. An analogous situation can also be pictured in the case of the post form $R_{if}^{(\mathrm{BDW})+}$ of the transition amplitude. Explicit calculations of the matrix elements $R_{if}^{(\mathrm{BDW})\pm}$ have been carried out by Belkić [21]. He has shown that the matrix elements $R_{if}^{(\mathrm{BDW})\pm}$ can be reduced to four-dimensional real numerical integrations from 0 to 1. The ensuing total cross sections in the BDW-4B method are obtained by a five-dimensional quadratures. It should be noted that the integrands in the prior and post forms have the functions $[\tau_k/(1-\tau_k)]^{i\nu_{P,T}}$ $(k = 1, 2)$ which originate from the standard integral representation of the two confluent hyper-geometric functions. These functions possess integrable branch-points singularities at $\tau_{1,2} = 0$ and $\tau_{1,2} = 1$, as well as simple poles at points $\tau_{1,2} = 0$. Therefore, the Cauchy regularization of the whole integrand should be performed before applying the usual Gauss–Legendre quadratures [21].

When computing differential cross sections, a very favorable computational circumstance occurs using the BDW-4B approximation in the prior form for $Z_P = 2$ or in the post version for $Z_T = 2$. In such a special case with the H^{2+} projectile impinging upon any two-electron target (or an arbitrary projectile Z_P and helium target), the Sommerfeld parameter $\nu_f = Z_T(Z_P - 2)/v$ or $\nu_f = Z_P(Z_T - 2)/v$ is zero in (6.2) or in (6.7), so that the Coulomb logarithmic phase factors $(vR - \boldsymbol{v}\cdot\boldsymbol{R})^{i\xi_T}$ or $(vR + \boldsymbol{v}\cdot\boldsymbol{R})^{i\xi_P}$ is the only $\boldsymbol{R}$-dependent function (without any phase in terms of ρ) in $T_{if}^{(\mathrm{BDW})-}$ or $T_{if}^{(\mathrm{BDW})+}$. In other words, the distorting function $\mathcal{L}^-(\boldsymbol{r}_i, \boldsymbol{r}_f)$ is reduced to the following form:

$$
\begin{aligned}
T_{if}^{(\mathrm{BDW})-}: \qquad \mathcal{L}_1(\boldsymbol{r}_i, \boldsymbol{r}_f) &= \mu_i^{-i\xi_T}\mathcal{N}^+(\xi_T)\,{}_1F_1(-i\xi_T, 1, ik_i r_f + i\boldsymbol{k}_i\cdot\boldsymbol{r}_f) \\
&\simeq (vR - \boldsymbol{v}\cdot\boldsymbol{R})^{i\xi_T} \\
\xi_T = 2\nu_T = 2Z_T/v \qquad (Z_P = 2\ ,\ &\text{any } Z_T)
\end{aligned}
\tag{6.15}
$$

and a similar simplification is obtained for $\mathcal{L}_2(\boldsymbol{r}_i, \boldsymbol{r}_f)$ via:

$$
\begin{aligned}
T_{if}^{(\mathrm{BDW})+}: \qquad \mathcal{L}_2(\boldsymbol{r}_i, \boldsymbol{r}_f) &= \mu_f^{-i\xi_P}\mathcal{N}^+(\xi_P)\,{}_1F_1(-i\xi_P, 1, ik_f r_i + i\boldsymbol{k}_f\cdot\boldsymbol{r}_i) \\
&\simeq (vR + \boldsymbol{v}\cdot\boldsymbol{R})^{i\xi_P}, \\
\xi_P = 2\nu_P = 2Z_P/v \qquad (Z_T = 2\ ,\ &\text{any } Z_P).
\end{aligned}
\tag{6.16}
$$

Under these particular circumstances, the computationally difficult and time-consuming Fourier–Bessel transform (as an integral over ρ-dependent transition amplitudes), is not needed in the BDW-4B method, since the angular distribution $(\mathrm{d}/\mathrm{d}\Omega)\,Q^{(\mathrm{BDW})-}$ or $(\mathrm{d}/\mathrm{d}\Omega)\,Q^{(\mathrm{BDW})+}$ can be obtained directly via

$$\frac{\mathrm{d}Q^{(\mathrm{BDW})-}}{\mathrm{d}\Omega} = \left|\frac{\mu}{2\pi} T_{if}^{(\mathrm{BDW})-}\right|^2 \qquad (Z_\mathrm{P} = 2, \ \text{any} \ Z_\mathrm{T}) \tag{6.17}$$

and

$$\frac{\mathrm{d}Q^{(\mathrm{BDW})+}}{\mathrm{d}\Omega} = \left|\frac{\mu}{2\pi} T_{if}^{(\mathrm{BDW})+}\right|^2 \qquad (Z_\mathrm{T} = 2, \ \text{any} \ Z_\mathrm{P}) \tag{6.18}$$

where μ is the reduced mass of P and T given by $\mu = M_\mathrm{P} M_\mathrm{T}/(M_\mathrm{P} + M_\mathrm{T})$. The BDW-4B method has first been formulated by Belkić [21] who illustrated this method for double electron capture in the He^{2+}–He collisions. Subsequently, the BDW-4B method has been applied by Mančev [54–57] to single electron capture by fast nuclei from helium-like targets.

7 The BCIS-4B method

Recall that the three-body continuum intermediate state (CIS-3B) approximation has been introduced by Belkić [58] for process (2.7). The CIS-3B method was aimed to treat asymmetric collisions, such that its prior and post versions are adapted for $Z_T \gg Z_P$ and $Z_P \gg Z_T$, respectively. This method satisfies the correct boundary condition only in the channel with the stronger potential [18,58]. In the channel with the weaker potential, the CIS-3B method uses the unperturbed state which does not have the proper asymptotic behavior for process (2.7). Such a drawback can be rectified via distortion of the unperturbed state from the entrance channel (which has a weaker potential) by an additional $\boldsymbol{R}$-dependent phase due to the electron–nucleus interaction at infinitely large distances. As a consequence, the correct boundary condition also becomes satisfied in the channel with the weaker potential. This leads to the three-body boundary-corrected intermediate state (BCIS-3B) method for single electron capture (2.7) in a general case with arbitrary nuclear charges Z_P and Z_T.

For a more complicated process, such as double electron capture (2.1), a proper extension of the BCIS-3B method is needed to treat four-body collisions. This generalization is known as the BCIS-4B method which has been formulated and implemented by Belkić [5]. The BCIS-4B method takes full account of the twofold electronic continuum intermediate states in one channel (entrance or exit, depending upon whether the prior or post form of the transition amplitudes is considered). The matrix element from the transition amplitudes in the prior and the post versions of the BCIS-4B method are [5]:

$$T_{if}^{(\mathrm{BCIS})-}(\boldsymbol{\eta}) = Z_{\mathrm{P}} N_{\mathrm{T}} \iiint \mathrm{d}\boldsymbol{s}_1 \mathrm{d}\boldsymbol{s}_2 \mathrm{d}\boldsymbol{R}\, \mathrm{e}^{i\boldsymbol{k}_i\cdot\boldsymbol{r}_i + i\boldsymbol{k}_f\cdot\boldsymbol{r}_f} \mathcal{L}_1(\boldsymbol{r}_i, \boldsymbol{r}_f) \times \varphi_f^*(\boldsymbol{s}_1, \boldsymbol{s}_2) \left(\frac{2}{R} - \frac{1}{s_1} - \frac{1}{s_2}\right) \varphi_i(\boldsymbol{x}_1, \boldsymbol{x}_2) \times {}_1F_1(i\nu_{\mathrm{T}}, 1, ivx_1 + i\boldsymbol{v}\cdot\boldsymbol{x}_1)\, {}_1F_1(i\nu_{\mathrm{T}}, 1, ivx_2 + i\boldsymbol{v}\cdot\boldsymbol{x}_2) \quad (7.1)$$

and

$$T_{if}^{(\mathrm{BCIS})+}(\boldsymbol{\eta}) = Z_{\mathrm{T}} N_{\mathrm{P}} \iiint \mathrm{d}\boldsymbol{x}_1 \mathrm{d}\boldsymbol{x}_2 \mathrm{d}\boldsymbol{R}\, \mathrm{e}^{i\boldsymbol{k}_i\cdot\boldsymbol{r}_i + i\boldsymbol{k}_f\cdot\boldsymbol{r}_f} \mathcal{L}_2(\boldsymbol{r}_i, \boldsymbol{r}_f) \times \varphi_f^*(\boldsymbol{s}_1, \boldsymbol{s}_2) \left(\frac{2}{R} - \frac{1}{x_1} - \frac{1}{x_2}\right) \varphi_i(\boldsymbol{x}_1, \boldsymbol{x}_2) \times {}_1F_1(i\nu_{\mathrm{P}}, 1, ivs_1 + i\boldsymbol{v}\cdot\boldsymbol{s}_1)\, {}_1F_1(i\nu_{\mathrm{P}}, 1, ivs_2 + i\boldsymbol{v}\cdot\boldsymbol{s}_2) \quad (7.2)$$

where the functions $\mathcal{L}_1(\boldsymbol{r}_i, \boldsymbol{r}_f)$ and $\mathcal{L}_2(\boldsymbol{r}_i, \boldsymbol{r}_f)$ are the same as those in (6.2) and (6.7), respectively. The two full Coulomb waves from (6.2) and (6.7) for the relative motion of heavy particles could, in principle, be kept in the calculations throughout. This would include the contributions of the order of or smaller than $1/\mu_i$ and $1/\mu_f$. Numerically, these latter contributions are negligibly small, since they amount to keeping all the terms that are of the order of or $<10^{-4}$ relative to 1. Of course, this is totally unnecessary within a consistent application of the eikonal approximation, in which the full Coulomb wave functions for the relative motions of heavy particles should be systematically replaced by their logarithmic Coulomb phase factors as in (6.3) and (6.8). Under such circumstances, the post and prior total cross section in the BCIS-4B methods are given by:

$$Q_{if}^{(\mathrm{BCIS})\pm}\left(a_0^2\right) = \int \mathrm{d}\boldsymbol{\eta} \left| \frac{R_{if}^{(\mathrm{BCIS})\pm}(\boldsymbol{\eta})}{2\pi v} \right|^2 \quad (7.3)$$

where $R_{if}^{(\mathrm{BCIS})+}$ and $R_{if}^{(\mathrm{BCIS})-}$ are independent of the inter-nuclear potential:

$$R_{if}^{(\mathrm{BCIS})-}(\boldsymbol{\eta}) = Z_{\mathrm{P}} N_{\mathrm{T}} \iiint \mathrm{d}\boldsymbol{s}_1 \mathrm{d}\boldsymbol{s}_2 \mathrm{d}\boldsymbol{R}\, \mathrm{e}^{i\boldsymbol{k}_i\cdot\boldsymbol{r}_i + i\boldsymbol{k}_f\cdot\boldsymbol{r}_f} \times (vR - \boldsymbol{v}\cdot\boldsymbol{R})^{-i\xi_{\mathrm{P}}} \varphi_f^*(\boldsymbol{s}_1, \boldsymbol{s}_2) \left(\frac{2}{R} - \frac{1}{s_1} - \frac{1}{s_2}\right) \varphi_i(\boldsymbol{x}_1, \boldsymbol{x}_2) \times {}_1F_1(i\nu_{\mathrm{T}}, 1, ivx_1 + i\boldsymbol{v}\cdot\boldsymbol{x}_1)\, {}_1F_1(i\nu_{\mathrm{T}}, 1, ivx_2 + i\boldsymbol{v}\cdot\boldsymbol{x}_2) \quad (7.4)$$

$$R_{if}^{(\mathrm{BCIS})+}(\boldsymbol{\eta}) = Z_{\mathrm{T}} N_{\mathrm{P}} \iiint \mathrm{d}\boldsymbol{x}_1 \mathrm{d}\boldsymbol{x}_2 \mathrm{d}\boldsymbol{R}\, \mathrm{e}^{i\boldsymbol{k}_i\cdot\boldsymbol{r}_i + i\boldsymbol{k}_f\cdot\boldsymbol{r}_f} \times (vR + \boldsymbol{v}\cdot\boldsymbol{R})^{-i\xi_{\mathrm{T}}} \varphi_f^*(\boldsymbol{s}_1, \boldsymbol{s}_2) \left(\frac{2}{R} - \frac{1}{x_1} - \frac{1}{x_2}\right) \varphi_i(\boldsymbol{x}_1, \boldsymbol{x}_2) \times {}_1F_1(i\nu_{\mathrm{P}}, 1, ivs_1 + i\boldsymbol{v}\cdot\boldsymbol{s}_1)\, {}_1F_1(i\nu_{\mathrm{P}}, 1, ivs_2 + i\boldsymbol{v}\cdot\boldsymbol{s}_2)\,. \quad (7.5)$$

It should be noted that in $R_{if}^{(\mathrm{BCIS})\pm}$ the electronic continuum intermediate states are included in the same way as in $R_{if}^{(\mathrm{BDW})\mp}$. The essential difference between $R_{if}^{(\mathrm{BDW})\mp}$ and $R_{if}^{(\mathrm{BCIS})\pm}$ lies in the perturbation potentials. In $R_{if}^{(\mathrm{BCIS})\mp}(\boldsymbol{\eta})$, these potentials are given by scalar operators $[Z_\mathrm{P}(2/R - 1/s_1 - 1/s_2)]$ and $[Z_\mathrm{T}(2/R - 1/x_1 - 1/x_2)]$, whereas in the case $R_{if}^{(\mathrm{BDW})\pm}(\boldsymbol{\eta})$ we have the sum of the two typical vectorial differential (gradient) operator potentials $\left[\sum_{k=1}^{2}\nabla_{s_k}\ln\varphi_f^*(\boldsymbol{s}_1,\boldsymbol{s}_2)\cdot\nabla_{x_k}\right]$ and $\left[\sum_{k=1}^{2}\nabla_{x_k}\ln\varphi_i(\boldsymbol{x}_1,\boldsymbol{x}_2)\cdot\nabla_{s_k}\right]$, which are familiar from the CDW-4B method.

Two alternative methods have been developed by Belkić [5] for calculation of the matrix elements in the BCIS-4B method. One of these gives the matrix elements $R_{if}^{(\mathrm{BCIS})\pm}(\boldsymbol{\eta})$ in terms of a three-dimensional numerical integration over real variables from 0 to 1. This method provides the basic quantities $R_{if}^{(\mathrm{BCIS})\pm}(\boldsymbol{\eta})$ in the form of the four-dimensional numerical quadratures over real variables. Both methods have been found to give the same numerical results [5].

Similarly to the BDW-4B method, it is also possible in the BCIS-4B method to alleviate altogether the cumbersome Fourier–Bessel transform, and thus perform direct computations of differential cross sections $(\mathrm{d}/\mathrm{d}\Omega)Q^{(\mathrm{BCIS})-}$ or $(\mathrm{d}/\mathrm{d}\Omega)Q^{(\mathrm{BCIS})+}$ for a special case $Z_\mathrm{T} = 2$ or $Z_\mathrm{P} = 2$, respectively. The only difference is that the particular case $Z_\mathrm{T} = 2$ or $Z_\mathrm{P} = 2$ relates to the post $(\mathrm{d}/\mathrm{d}\Omega)Q^{(\mathrm{BCIS})+}$ or prior $(\mathrm{d}/\mathrm{d}\Omega)Q^{(\mathrm{BCIS})-}$ angular distributions, respectively (the reverse assignment takes place in the BDW-4B method):

$$\frac{\mathrm{d}Q^{(\mathrm{BCIS})-}}{\mathrm{d}\Omega} = \left|\frac{\mu}{2\pi}T_{if}^{(\mathrm{BCIS})-}\right|^2 \qquad (Z_\mathrm{T} = 2, \quad \text{any} \quad Z_\mathrm{P}), \tag{7.6}$$

$$\frac{\mathrm{d}Q^{(\mathrm{BCIS})+}}{\mathrm{d}\Omega} = \left|\frac{\mu}{2\pi}T_{if}^{(\mathrm{BCIS})+}\right|^2 \qquad (Z_\mathrm{P} = 2, \quad \text{any} \quad Z_\mathrm{T}). \tag{7.7}$$

Double electron capture (2.1) has also been investigated by Purkait [59] and Purkait et al. [60]. They used the unperturbed wave function Φ_i for the initial scattering state which, therefore, disregards the correct boundary condition in the entrance channel, in the case of the general values of Z_T and Z_P. Specifically, only for $Z_\mathrm{T} = 2$ and any Z_P, with no residual Coulomb potential $V_i^\infty = Z_\mathrm{P}(Z_\mathrm{T} - 2)/R = 0$, the unperturbed state Φ_i from Refs. [59,60] possesses the correct asymptotic behavior, because exclusively in this particular case we have $\Phi_i^+ = \Phi_i$. In the exit channel the scattering wave function from Refs. [59,60] is adequate, and it coincides with the corresponding state from the BCIS-4B method [5]. Had the correct boundary conditions for the entrance channel also been included by Purkait [59] and Purkait et al. [60] from the outset in the general case of arbitrary values of Z_P and Z_T for process (2.1), these authors would have rediscovered the BCIS-4B method of Belkić [5] according to (7.1) and (7.2). Explicit computations from Refs. [59,60] were concerned with double charge exchange in the He^{2+}–He, Li^{3+}–He and B^{5+}–He collisions. In this particular case with a helium target ($Z_\mathrm{T} = 2$), the Sommerfeld parameter $\nu_f = Z_\mathrm{P}(Z_\mathrm{T} - 2)$ becomes zero which leads to $\mathcal{N}^{-*}(\nu_f)\,{}_1F_1(-i\nu_f, 1, ik_f r_i + i\boldsymbol{k}_f\cdot\boldsymbol{r}_i) = 1$ in $\mathcal{L}_1(\boldsymbol{r}_i, \boldsymbol{r}_f)$ from (6.2). Fortuitously, this implies that $\Phi_i^+ = \Phi_i$ in which case the matrix elements from Refs. [59,60] coincides

with (7.1) from the BCIS-4B method. In the computations from Refs. [59,60] the remaining full Coulomb wave function $\chi_{\rm Coul} \equiv \mathcal{N}^{+}(\nu)_1F_1(-i\nu, 1, ik_i r_f + i\boldsymbol{k}_i \cdot \boldsymbol{r}_f)$ with $\nu = Z_{\rm P}Z_{\rm P}/v$ for the relative motion of heavy particles was used instead of its consistent eikonal expressions $\chi_{\rm eik} \equiv \mu_i^{i\nu} \exp\left[i\nu \ln(vR - \boldsymbol{v}\cdot\boldsymbol{R})\right]$. Nevertheless, as already stated, the difference between the corresponding results for the total cross sections obtained using the said full Coulomb wave and its eikonal limit, i.e. $\chi_{\rm Coul}$ and $\chi_{\rm eik}$ within the BCIS-4B method for double electron capture in e.g. the $Z_{\rm P}$–He collisions should be in the 3rd or 4th decimal places. The two such explicit sets of the total cross sections in the BCIS-4B method for the He^{2+}–He collisions based upon $\chi_{\rm eik}$ and $\chi_{\rm Coul}$ in the entrance channel have been published by Belkić [5] and Purkait [59], respectively. The results from these two studies should be indistinguishable from each other within the accuracy 10^{-3}–10^{-4}. However, this is not the case, pointing to the existence of some computational errors in the work of Purkait [59], given the veracity of the results of Belkić [5] from the BCIS-4B method, which has been thoroughly checked to yield the identical cross sections using two completely different methods for all the matrix elements.

8 The CB1-4B method

Numerous investigations and comparisons with experiments have confirmed that the CB1-3B method is an accurate theory for rearrangement collisions at intermediate and high impact energies [61–68]. Therefore, it is reasonable to extend this approximation to four-body collisions with one or two active electrons. Such an extension for double capture has been done by Belkić [69,70] through the introduction of the CB1-4B method. The transition amplitudes in the CB1-4B method for double charge exchange within the prior $\left(T_{if}^{-}\right)$ and the post $\left(T_{if}^{+}\right)$ forms can be taken from Ref. [70] without the term $(v\rho)^{2iZ_{\rm P}Z_{\rm T}/v}$:

$$T_{if}^{\pm}(\boldsymbol{\eta}) = \int \mathrm{d}\boldsymbol{R} \mathrm{e}^{\mp 2i\boldsymbol{q}_{\rm P,T}\cdot\boldsymbol{R}} (vR + \boldsymbol{v}\cdot\boldsymbol{R})^{-i\xi} \mathcal{F}^{\pm}(\boldsymbol{R}), \tag{8.1}$$

$$\mathcal{F}^{-}(\boldsymbol{R}) = Z_{\rm P} \int\int \mathrm{d}\boldsymbol{s}_1 \mathrm{d}\boldsymbol{s}_2 \varphi_f^{*}(\boldsymbol{s}_1, \boldsymbol{s}_2) \mathrm{e}^{-i\boldsymbol{v}\cdot(\boldsymbol{s}_1+\boldsymbol{s}_2)} \times \left(\frac{2}{R} - \frac{1}{s_1} - \frac{1}{s_2}\right) \varphi_i(\boldsymbol{x}_1, \boldsymbol{x}_2), \tag{8.2}$$

$$\mathcal{F}^{+}(\boldsymbol{R}) = Z_{\rm T} \int\int \mathrm{d}\boldsymbol{x}_1 \mathrm{d}\boldsymbol{x}_2 \varphi_f^{*}(\boldsymbol{s}_1, \boldsymbol{s}_2) \mathrm{e}^{-i\boldsymbol{v}\cdot(\boldsymbol{x}_1+\boldsymbol{x}_2)} \times \left(\frac{2}{R} - \frac{1}{x_1} - \frac{1}{x_2}\right) \varphi_i(\boldsymbol{x}_1, \boldsymbol{x}_2), \tag{8.3}$$

where $\xi = 2(Z_{\rm T} - Z_{\rm P})/v$. These expressions are based upon (6.4) as well as:

$$\begin{aligned} \boldsymbol{k}_i \cdot \boldsymbol{r}_i + \boldsymbol{k}_f \cdot \boldsymbol{r}_f &= \boldsymbol{q}_{\rm P} \cdot (\boldsymbol{s}_1 + \boldsymbol{s}_2) + \boldsymbol{q}_{\rm T} \cdot (\boldsymbol{x}_1 + \boldsymbol{x}_2) \\ &= -2\boldsymbol{q}_{\rm P} \cdot \boldsymbol{R} - \boldsymbol{v} \cdot (\boldsymbol{x}_1 + \boldsymbol{x}_2) = 2\boldsymbol{q}_{\rm T} \cdot \boldsymbol{R} - \boldsymbol{v} \cdot (\boldsymbol{s}_1 + \boldsymbol{s}_2), \end{aligned} \tag{8.4}$$

$$2\boldsymbol{q}_{\mathrm{P}} = +\boldsymbol{\eta} - v^{+}\hat{\boldsymbol{v}}, \quad 2\boldsymbol{q}_{\mathrm{T}} = -\boldsymbol{\eta} - v^{-}\hat{\boldsymbol{v}}, \quad \boldsymbol{q}_{\mathrm{P}} + \boldsymbol{q}_{\mathrm{T}} = -\boldsymbol{v}, \tag{8.5}$$

$$v^{+} = v + \frac{E_f - E_i}{v}, \quad v^{-} = v - \frac{E_f - E_i}{v}. \tag{8.6}$$

The vector of the incident velocity $\boldsymbol{v}$ is chosen along the Z-axis, i.e. $\hat{\boldsymbol{v}} = (0, 0, 1)$, whereas the vector $\boldsymbol{\eta}$ is the transverse momentum transfer in the XOY plane:

$$\boldsymbol{\eta} = (\eta \cos\phi_\eta, \eta \sin\phi_\eta, 0), \qquad \boldsymbol{\eta} \cdot \boldsymbol{v} = 0. \tag{8.7}$$

A complete analytical calculation of the matrix elements $T_{if}^{\pm}(\boldsymbol{\eta})$, as a two-dimensional integral, has been carried out by Belkić [70]. The method used is general in the sense that it can be applied to hetero-nuclear (asymmetric) [70], as well as homo-nuclear (symmetric) [69] collisions in which double charge exchange occurs. This has been substantiated for the symmetric He^{2+}–He collision, for which the algorithm of Belkić [70] reproduced exactly the results from the corresponding previous study [69]. This cross-validation is important, since Belkić [69] presented a completely different way of calculating the matrix elements. It should be mentioned that the partial wave analysis of the transition amplitude in the CB1-4B method has also been performed for double electron capture in collisions of alpha particles and helium [71]. If the necessary convergence over the partial waves has been achieved, the numerical results of Gulyás and Szabo [71] would be the same as those obtained without the partial wave analysis. However, this is not the case (as will be shown later in Fig. 4), possibly due to the inclusion of merely three partial waves and/or because of some computational errors made by Gulyás and Szabo [71].

9 Comparison between theories and experiments

9.1 Double electron capture into the ground state

We first analyze the total cross sections in the CDW-4B method for double electron capture from He by fast H^+ and He^{2+} ions:

$$H^+ + He(1s^2) \longrightarrow H^-(1s^2) + He^{2+}, \tag{9.1}$$

$$He^{2+} + He(1s^2) \longrightarrow He(1s^2) + He^{2+}. \tag{9.2}$$

In order to investigate the sensitivity of the prior and post forms of the total cross sections to the choice of the ground-state wave functions for He and H^-, we employ four two-electron functions: a one-parameter uncorrelated functions of Hylleraas [72], a radially correlated two-parameter orbital of Silverman et al. [73], a three-parameter function of Green et al. [74], and a four-parameter function of Löwdin [75]. As shown by Belkić and Mančev [7], the post–prior discrepancy for reaction (9.1) for all four wave functions is within at most 40% at impact energies where the CDW-4B method is expected to be most adequate ($E \geq 100\,\mathrm{keV}$). In the case of the wave function of Löwdin [75], the difference between the prior and post cross section does not exceed 20% at $E \geq 100\,\mathrm{keV}$.

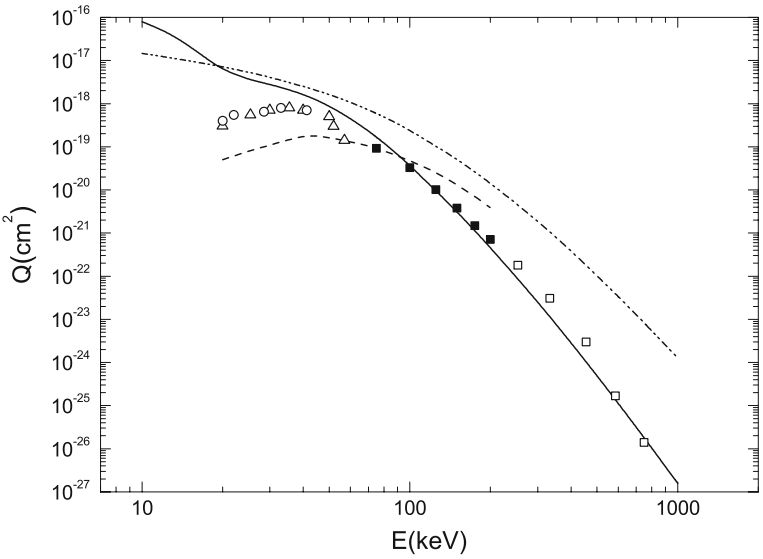

Fig. 1 Total cross sections Q as a function of the incident energy E for process (9.1). Theory: *full curve* (CDW-4B method [7]), *doubly-chained curve* (CB1-4B method: present results) and *dashed curve* (AO method [77]). Experiment: *filled square* [80], *open square* [81], *open triangle* [82,83] and *open circle* [84]

Total cross sections in their post forms for process (9.1) are given in Figs. 1 and 2 using the wave functions of Hylleraas [72] for the initial and final helium-like states. It has been verified in the CDW-4B method [76] that the high-energy cross sections computed using the orbitals of Silverman et al. [73], Green et al. [74] and Löwdin [75] are very close to those associated with the wave function of Hylleraas [72]. The cross sections of the CDW-4B method are seen in Fig. 1 to be in excellent agreement with the available experimental data at impact energies $E \geq 100$ keV. However, the present results of the CB1-4B method also given in Fig. 1, markedly overestimate the experimental data. The cross sections from the three-state two-center close coupling atomic orbital (AO) method used by Lin [77] considerably underestimate the measured data at lower energies ($E \leq 45$ keV), with precisely the reversed pattern above 120 keV.

In Fig. 2 the present cross sections obtained using the CB1-4B and the four-body first-order Jackson–Schiff (JS1-4B) methods are compared with each other for process (9.1). As can be seen from this figure, noticeable differences exist between these two methods below 200 keV pointing to the importance of the correct boundary conditions that are preserved in the CB1-4B method and ignored in the JS1-4B method. Also shown in Fig. 2 are the earlier results of Gerasimenko [78,79]. He aimed at using the JS1-4B method, but his results are wrong and, as such, denoted by JS1$^{\#}$-4B to avoid confusion with the corresponding exact results from the JS1-4B method.

We can conclude that, in the case of reaction (9.1) at impact energies $E \geq 100$ keV, the CDW-4B method is not strongly dependent upon the choice of the bound-state wave functions from Refs. [72–75]. Hence, the simplest one-parameter orbital of Hylleraas [72] can confidently be used in subsequent applications regarding process (9.1).

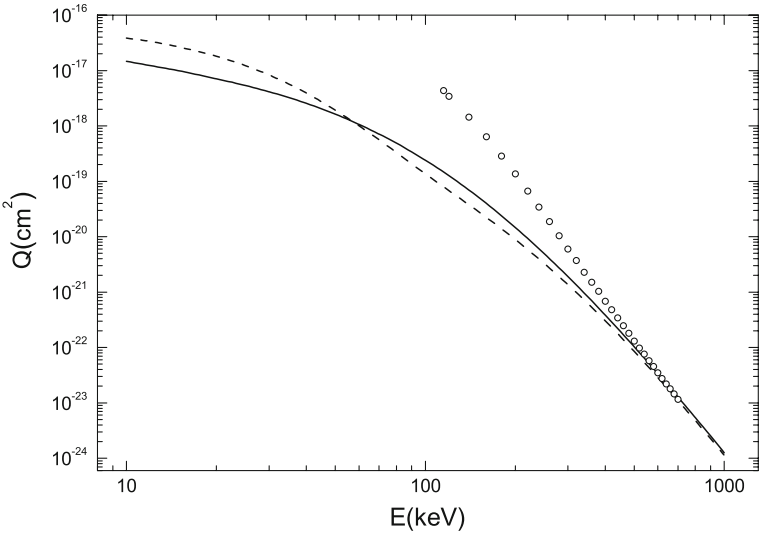

Fig. 2 Total cross sections Q as a function of the incident energy E for process (9.1). Theory: *full curve* (CB1-4B: present results), *dashed curve* (JS1-4B method: present results) and *open circles* (JS1$^{\#}$-4B method [78,79])

At energies $E \geq 100\,\text{keV}$, where the CDW-4B method is assessed to be adequate, the prior and post cross sections are in satisfactory mutual agreement and, furthermore, they provide an excellent interpretation of the existing experimental data on the H^+–He double charge exchange.

The cross sections for process (9.2) in the CDW-4B method have first been reported in Refs. [21,22]. There is no post–prior discrepancy for this reaction, so that $Q_{if}^{-} = Q_{if}^{+} \equiv Q_{if}$. It has been found by Belkić et al. [22] that the dependence of the total cross sections for the He^{2+}–He collisions upon the bound-state wave functions is not strong and, therefore, similar to that in the H^+–He collisions. The first-order theories for process (9.2) are illustrated in Figs. 3, 4, 5, 6, 7, 8, 9 using the CB1-4B, BDW-4B, BCIS-4B, CDW-4B1 and CDW-EIS-4B1 methods. Figure 10 presents certain additional results with approximate second-order contributions from a distorted wave perturbation expansion [6] which is not the series of Dodd and Greider [23]. Surprisingly, as seen in Fig. 3, the results from the CDW-4B1 method [21,22] for process (9.2) do not reproduce most of the experimental data, except those at the two largest energies 4 and 6 MeV.

In the same Fig. 3 for process (9.2) we also give the cross sections from the CB1-4B method [69,70]. Below 1.5 MeV, the CDW-4B method agrees well with the experimental data, but gives too large cross sections above 1.5 MeV. Fortuitously, and only for the particular process (9.2), where $Z_P = 2 = Z_T$, the CB1-4B and JS1-4B method coincide with each other. However, since in this special case, both the initial and final Coulomb phases for the relative motions of the nuclei disappear altogether, the channel wave functions in the BK1-4B method also possess the proper asymptotic behaviors. Nevertheless, the BK1-4B method still disobeys the correct boundary conditions, even

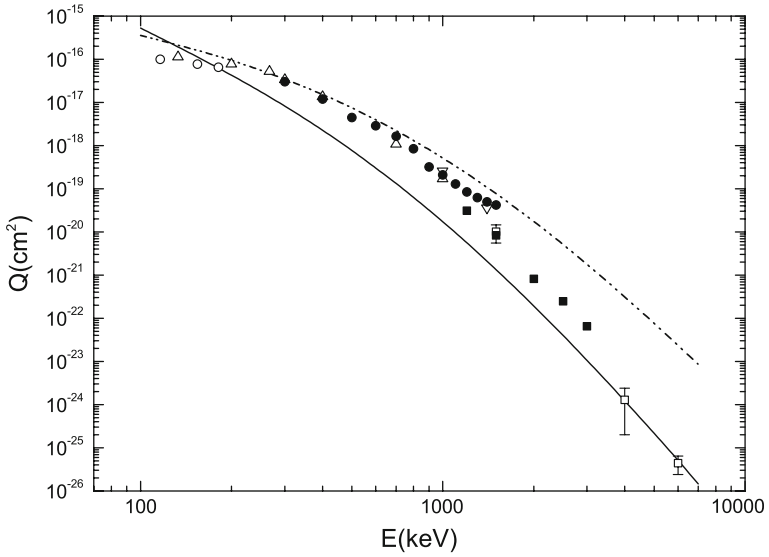

Fig. 3 Total cross sections Q as a function of the incident energy E for process (9.2). Theory: *full curve* (CDW-4B method [21]) and *doubly-chained curve* (CB1-4B method [69,70]). Experiment: *open square* [85], *open circle* [86,87], *open down triangle* [88], *open up triangle* [89], *open square* [90] and *filled circle* [91]

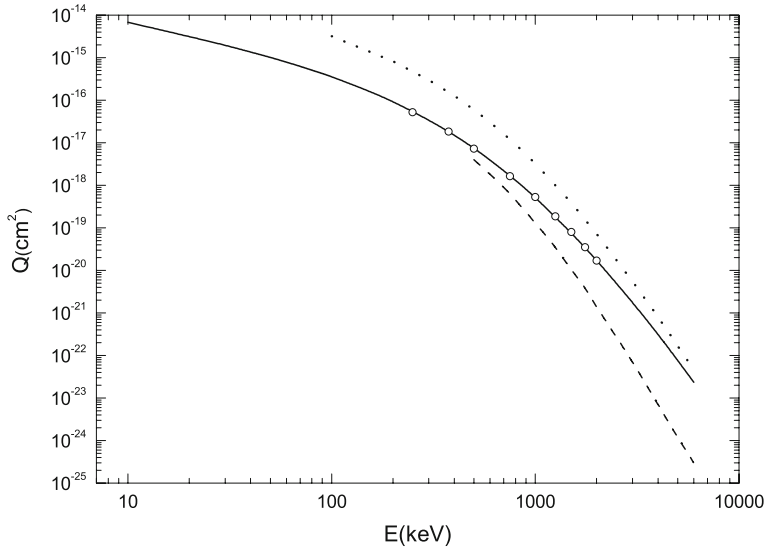

Fig. 4 Total cross sections Q as a function of the incident energy E for process (9.2). Theory: *full curve* (CB1-4B method: present results), *dashed curve* (CB1$^{\#}$-4B method [71]), *dotted curve* (BK1-4B: present results) and *open circles* (JS1-4B method [92,93])

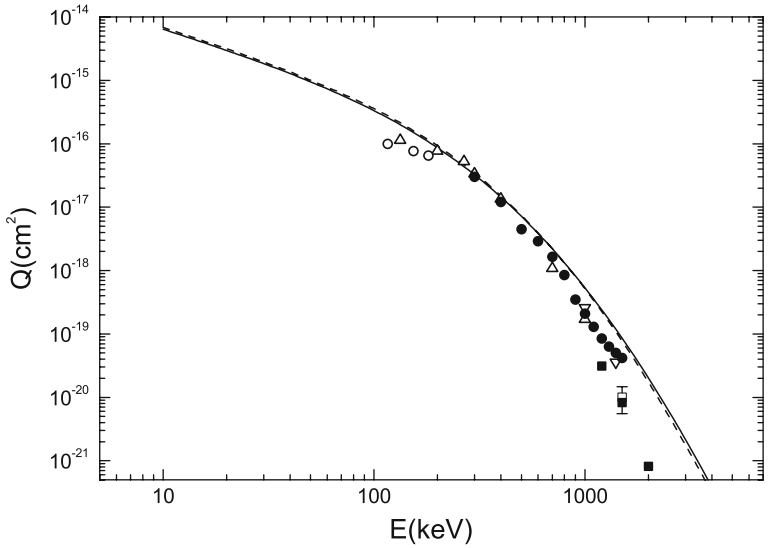

Fig. 5 Total cross sections Q as a function of the incident energy E for process (9.2). Theory: *dashed curve* (CB1-4B method without perturbation O_i [69,70]) and *full curve* (CB1-4B method with perturbation O_i [70]). Experiment: filled square [85], *open circle* [86,87], *open down triangle* [88], *open up triangle* [89], *open square* [90] and *filled circle* [91]

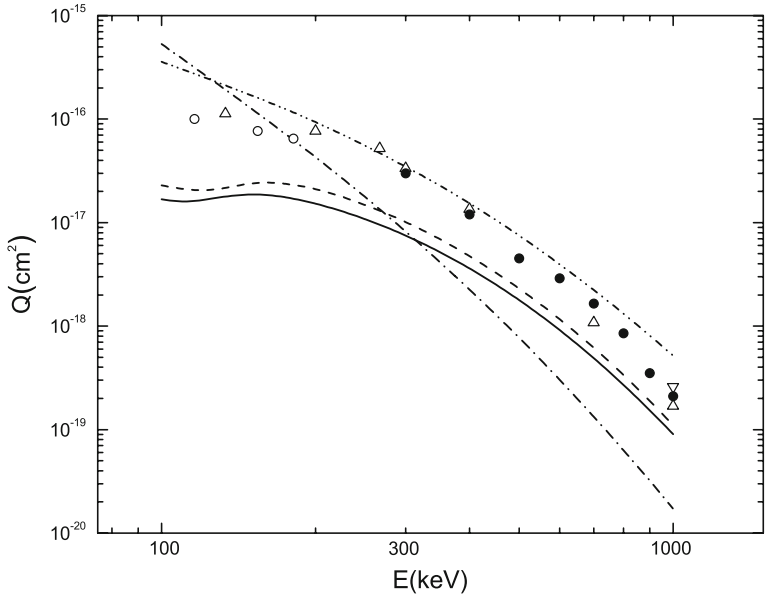

Fig. 6 Total cross sections Q as a function of the incident energy E for process (9.2). Theory: *doubly-chained curve* (CB1-4B method [69,70]), *dashed curve* (BCIS-4B method [5]), *full curve* (BDW-4B method [21]) and *singly-chained curve* (CDW-4B method [21]). Experiment: *open circle* [86,87], *open down triangle* [88], *open up triangle* [89] and *filled circle* [91]

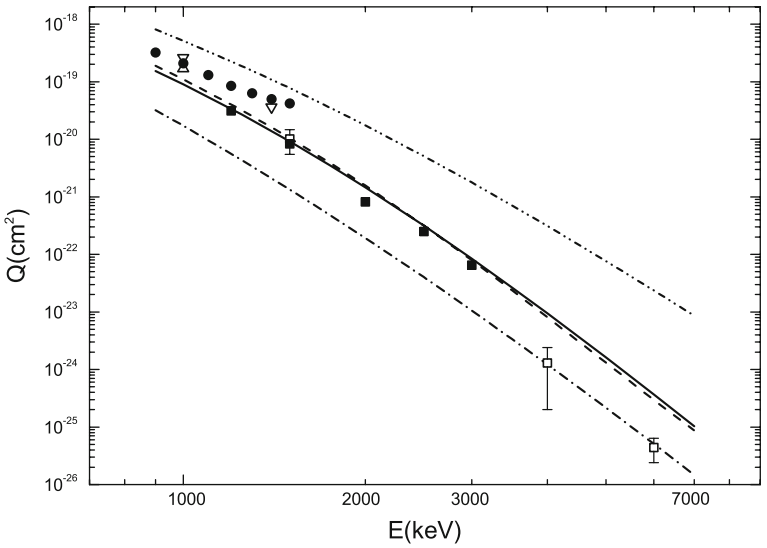

Fig. 7 Total cross sections Q as a function of the incident energy E for process (9.2). Theory: *doubly-chained curve* (CB1-4B method [69,70]), *dashed curve* (BCIS-4B method [5]), *full curve* (BDW-4B method [21]) and *singly-chained curve* (CDW-4B method [21]). Experiment: *filled square* [85], *open down triangle* [88], *open up triangle* [89], *open square* [90] and *filled circles* [91]

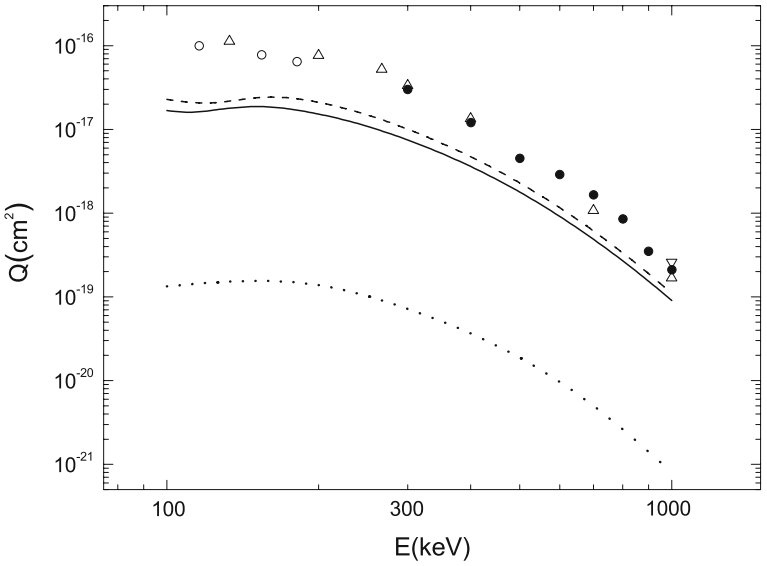

Fig. 8 Total cross sections Q as a function of the incident energy E for process (9.2). Theory: *dashed curve* (BCIS-4B method [5]), *full curve* (BDW-4B method [21]) and *dotted curve* (CDW-EIS-4B method [6]). Experiment: *open circle* [86,87], *open down triangle* [88], *open up triangle* [89] and *filled circle* [91]

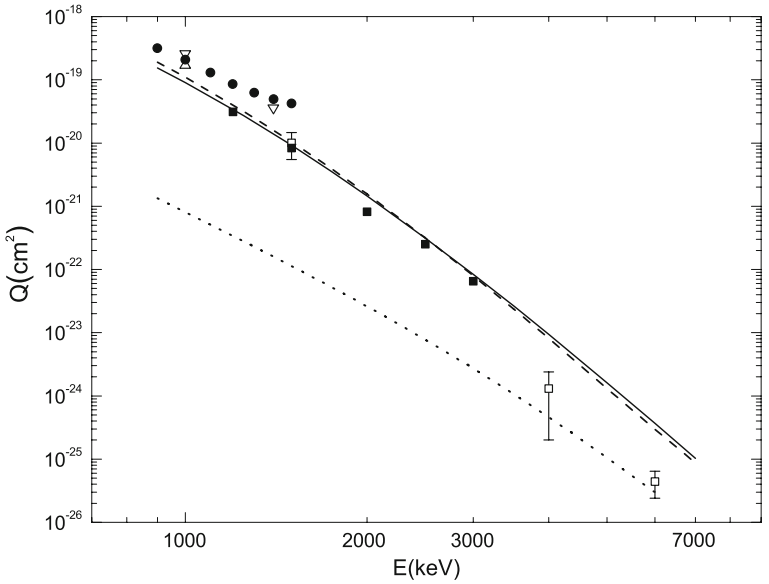

Fig. 9 Total cross sections Q as a function of the incident energy E for process (9.2). Theory: *dashed curve* (BCIS-4B method [5]), *full curve* (BDW-4B method [21]) and *dotted curve* (CDW-EIS-4B method [6]). Experiment: *filled square* [85], *open down triangle* [88], *open up triangle* [89], *open square* [90] and *filled circles* [91]

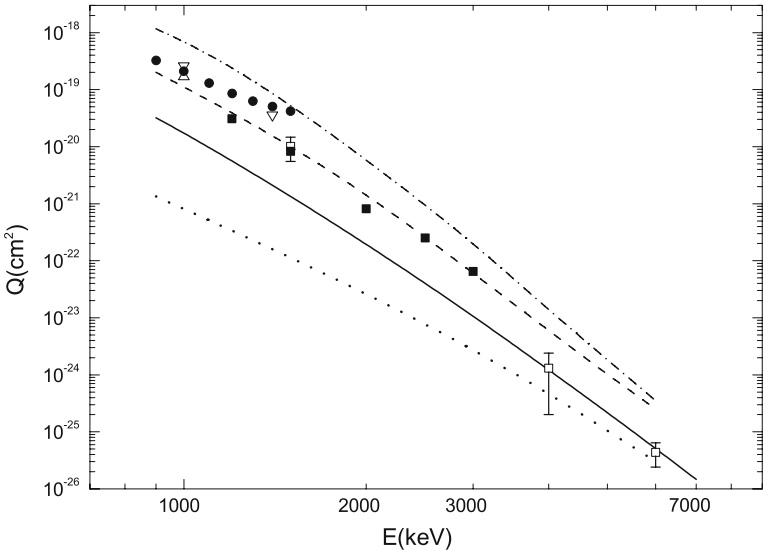

Fig. 10 Total cross sections Q as a function of the incident energy E for process (9.2). Theory: *full curve* (CDW-4B1 method [6,21]) *dashed curve* (CDW-4B2 method [6]), *dotted curve* (CDW-EIS-4B1 method [6]) and *singly-chained curve* (CDW-EIS-4B2 method [6]). Experiment: *filled square* [85], *open down triangle* [88], *open up triangle* [89], *open square* [90] and *filled circles* [91]

in the case of process (9.2), due to the appearance of the inadequate perturbation potentials. For example, in the exit channel the perturbation potential within the BK1-4B method has only the long-range interactions $Z_T(-1/x_1 - 1/x_2)$ instead of the physical short-range potential $Z_T(2/R - 1/x_1 - 1/x_2)$, which is required by the asymptotic convergence problem [8]. Therefore, the importance of the correct boundary conditions can also be inferred by comparing the CB1-4B and BK1-4B methods. Moreover, such a comparison would reveal the relative importance of the contributions from the terms $Z_T(-1/x_1 - 1/x_2)$ and $2Z_T/R$. This is illustrated in Fig. 4, where the cross sections of the BK1-4B method are seen to markedly overestimate the corresponding results from the CB1-4B method. Also shown in Fig. 4 are the results of Gulyás and Szabo [71] who used the partial wave analysis within the CB1-4B method. Their results markedly underestimate the true cross sections of the CB1-4B method [69,70], and this discrepancy increases when the energy is augmented, indicating that the three partial waves used in Ref. [71] are totally insufficient for achieving convergence. It is well-known that the number of partial waves needed for convergence increases significantly with increased impact energy, and this is at variance with keeping only three partial waves throughout, as done by Gulyás and Szabo [71]. The erroneous data given by Gulyás and Szabo [71] are denoted by CB1$^{\#}$-4B in Fig. 4 in order to avoid confusion with the corresponding exact cross sections from the CB1-4B method obtained by Belkić [69,70]. Note that the earlier findings from the CB1-4B method reported by Gerasimenko and Rosentsveig [92,93] are seen in Fig. 4 to be in perfect agreement with the corresponding results of Belkić [69,70].

In Fig. 5 comparison is made between the results from the CB1-4B method [69] with and without the perturbation O_i for process (9.2). This additional term in the perturbation potential is defined by:

$$(E_i - h_i)\varphi_i \equiv O_i \tag{9.3}$$

where h_i is the target electronic Hamiltonian. Obviously, the term O_i is equal to zero only for the exact eigen-solutions $\varphi_i(\boldsymbol{x}_1, \boldsymbol{x}_2) \equiv \varphi_i$ and E_i of h_i. However, since these latter solutions are unavailable, the term O_i should, in principle, be kept as suggested by Belkić [69] within the CB1-4B method. It is seen in Fig. 5 that the contribution of the perturbation O_i is very small and, as such, can be neglected throughout.

One of the inadequacies of the CDW-4B1 method is the use of unnormalized total scattering wave functions in both the entrance and exit channels. Of course, the same drawback of the CDW-3B method is also encountered for single charge exchange (2.7) [20], but without a significant consequence at impact energies satisfying the usual validity condition [8]:

$$\text{Incident energy } E(\text{keV/amu}) \geq 80 \max\{|E_i|, |E_f|\}, \tag{9.4}$$

where E_i and E_f are the initial and the final orbital energies of the captured electron, respectively.[1] The discrepancy between the CDW-4B1 method and experiments for

[1] According to (9.4), the expected limit of the validity of the CDW-4B1 method for a He^{2+} projectile is 0.45 MeV, whereas for a Li^{3+} ion impact it is above 2 MeV, and for a B^{5+} projectile it is above 9.7 MeV.

reaction (9.2) may indicate that the same type of inadequacies invoked in theories of rearrangement collisions could be more serious for double than for single charge exchange. Total cross sections for high-energy two-electron transfer are smaller than the corresponding results for one electron capture by at least two orders of magnitude. Therefore, it is not surprising that double charge exchange, as a much weaker effect than single electron transfer, appears to be very sensitive to any (even apparently small) inadequacies of the theory. Nevertheless, this normalization problem is not expected to be the main cause for the lack of agreement between the CDW-4B1 method and experiment below 4 MeV in Fig. 6. This could be inferred from the work of Martínez et al. [6]. Their results from the CDW-EIS-4B1 method (which uses the normalized eikonal scattering wave function in the entrance channel) underestimate both the experiments and the CDW-4B1 method for the same process (9.2), as seen in Figs. 8, 9, 10.

As was initially conjectured by Belkić et al. [22], an alternative reason for the fact that the CDW-4B1 method is satisfactory only at the highest energies (4 and 6 MeV) in Fig. 3 could be neglect of the second-order contribution from a perturbation series. Subsequently, Martínez et al. [6] used the sum of the T-matrix element from the CDW-4B1 method and an approximate on-shell second-order term from a perturbation expansion. They called the sum of these two latter T-matrix elements the four-body second-order continuum distorted wave (CDW-4B2) approximation. The usual eikonalization of the two full electronic continua in the entrance channel introduces a further approximation to the CDW-4B2 method known as the four-body second-order continuum distorted wave eikonal initial state (CDW-EIS-4B2) method [6]. Recall that the CDW-4B1 and CDW-EIS-4B1 methods are the first-orders to the perturbation series expansion of Dodd–Greider [23] without disconnected diagrams. Likewise, the proper CDW-4B2 and CDW-EIS-4B2 methods, as the second-orders to the same perturbation development of Dodd–Greider [23], would be obtained by including the second terms in this series. This is not what has been done by Martínez et al. [6]. Instead, they added a second-order propagator from an ordinary distorted wave expansion (with disconnected diagrams) to the transition T-operator of the CDW-4B1 method. Such a mixing of two terms from two different series with connected and disconnected diagrams is obviously inconsistent. As a consequence, acronyms CDW-4B2 and CDW-EIS-4B2 used by Martínez et al. [6] are misleading, since they do not refer to the second-orders of the Dodd–Greider series [23], as opposed to what one would be inclined to think by extrapolating the terminology with the CDW-4B1 and CDW-EIS-4B1 methods to the next (second) order in the expansion. For this reason in the conclusion to the two recent state-of-the-art reviews [2,3], the second-order model of Martínez et al. [6] was called the 'augmented continuum distorted wave method' and the 'augmented continuum distorted wave eikonal initial state method'. Likewise, hereafter we shall interchangeably use the abbreviations CDW-4B2 and 'augmented CDW-4B' (as well as CDW-EIS-4B2 and 'augmented CDW-EIS-4B'). However, the reader should always bear in mind the mentioned remark about the genuine second-order Dodd–Greider methods [23], especially in interpreting the results of comparisons between the CDW-4B1 and CDW-4B2 methods on the one hand, as well as between the CDW-EIS-4B1 and CDW-EIS-4B2 methods on the other hand.

The CDW-4B2 method yields the cross sections that agree favorably with most of the available experimental data in Fig. 10, except at 4 and 6 MeV (precisely the reverse pattern relative to the CDW-4B1 method). However, as seen in Fig. 10, the CDW-EIS-4B2 method gives the results that overestimate both the cross sections from the CDW-4B2 method and the experimental data for process (9.2). Regarding the CDW-EIS-4B1 method, Figs. 8 and 9 show that throughout the interval 100–3000 keV, $Q_{if}^{(\mathrm{CDW-EIS-4B1})}$ markedly underestimates the experimental data. For example, this underestimation is by 2–3 orders of magnitude in the range 100–2000 keV. This latter energy range is well within the expected validity domain of the CDW-EIS-4B1 method. On the other hand, in Fig. 10, the cross sections $Q_{if}^{(\mathrm{CDW-EIS-4B2})}$ overestimate considerably all the available experimental data in the whole range under consideration. In particular, at impact energies 100–1000 keV, the values of the ratio $Q_{if}^{(\mathrm{CDW-EIS-4B2})}/Q_{if}^{(\mathrm{CDW-EIS-4B1})}$ obtained by Martínez et al. [6] are enormous, ranging from 10^3 to 10^4.

The same on-shell Green propagator for a second-order contribution has also been used within the impulse approximation (IA) by Gravielle and Miraglia [94] for process (9.2). They omitted the first-order IA, but this is unjustified as they have not shown that this ignored term is indeed negligible. Moreover, such an omission is not supported by the CDW-4B2 method, which contains a significant contribution from the corresponding first-order term provided by the CDW-4B1 method, as seen via the full and dashed curves in Fig. 10. It is pertinent to recall that the IA for three- and four-body collisions does not obey the correct boundary conditions. This most serious drawback has been rectified by Belkić with the emergence of the three- and four-body Reformulated Impulse Approximation (RIA-3B, RIA-4B) [95–98].

Overall, as opposed to single electron capture, it is physically plausible that the second-order term in a perturbation expansion could play an important role for double electron capture, since in this latter process two electrons participate actively in the collision. This is evidenced by large differences between the CDW-4B1 and CDW-4B2 methods, on the one hand, and between the CDW-EIS-4B1 and CDW-EIS-4B2 methods, on the other hand.

These initial assessments of the second-order terms in a perturbation series are encouraging. Nevertheless, it would be very important to extend such computations by including both the on- and off-shell second-order contributions in the CDW-4B2 and CDW-EIS-4B2 methods for process (9.2). Furthermore, it would be indispensable to assess the convergence rate in the spectral representation of the Green function from a second-order propagator. This latter spectral representation from Martínez et al. [6] is inconclusive, as it takes into account only the two hydrogen-like ground states centered on the projectile and target nucleus, without the necessary assessment of the contribution from any of the other, ignored intermediate states.

Further, as can be seen from Figs. 6, 7, 8, 9, the BCIS-4B and BDW-4B methods yield very similar values for the displayed total cross sections. These two approximations use normalized scattering wave functions in one channel. The total cross sections from the BCIS-4B and BDW-4B methods are much smaller that those from the CB1-4B method throughout the energy range under consideration. For example, the difference between the findings of the BDW-4B and CB1-4B methods increases

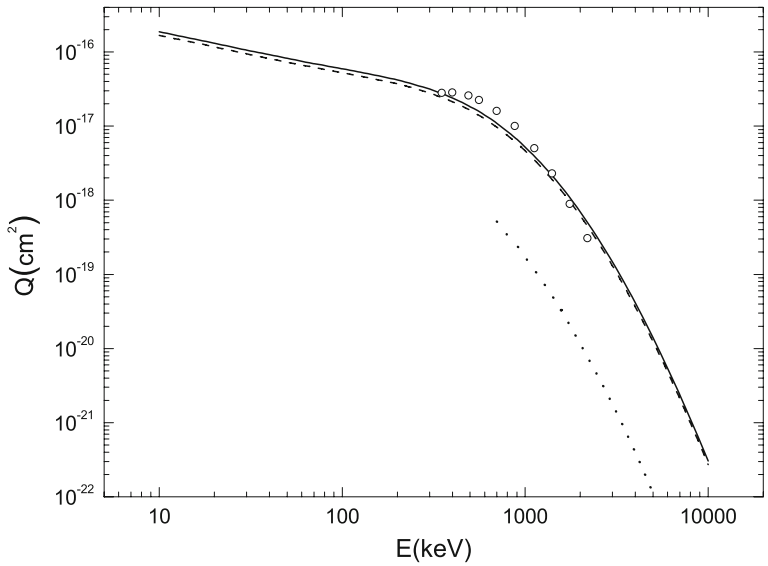

Fig. 11 Total cross sections Q as a function of the incident energy E for process (9.5). Theory: *dashed curve* (prior CB1-4B method [70]), *full curve* (post CB1-4B method [70]) and *dotted curve* (CDW-EIS-4B method [100]). Experiment: *open circle* [99]

as the impact energy is augmented, reaching two orders of magnitude at 6 MeV. Importantly, the BDW-4B and BCIS-4B methods are in good agreement with most of the available experimental data even without any second-order term from a distorted wave series.[2] However, at the two largest energies (4 and 6 MeV), the BDW-4B and BCIS-4B methods are seen in Fig. 7 to overestimate the measurements.

Next, we analyze the results of Belkić [70] obtained by means of the CB1-4B method for the following asymmetric reaction:

$$^7\mathrm{Li}^{3+} + {}^4\mathrm{He}(1s^2) \longrightarrow {}^7\mathrm{Li}^{+}(1s^2) + {}^4\mathrm{He}^{2+}. \tag{9.5}$$

The results for the total cross sections in both the post and prior versions for process (9.5) are depicted in Fig. 11. As can be seen from this figure, the post cross sections are slightly larger than the prior ones. The post–prior discrepancy appears to be somewhat more pronounced at lower than at higher energies. A comparison between the CB1-4B method and the experimental data of Shah and Gilbody [99] is also shown in Fig. 11. The results from the CB1-4B method are seen to be in satisfactory agreement with the experimental data. Thus, considering only the $1s^2 \longrightarrow 1s^2$ transition in process (9.5), it follows that the CB1-4B method compares more favorably with the measurement than the corresponding CDW-4B method, as evidenced by Figs. 6 and 11.

[2] Incidently, this casts doubt on the CDW-EIS-4B1 method which has been claimed [6] to be inadequate for double charge exchange because of neglect of the second-order propagator in the expansion of the total Green operator for the whole system.

The total cross sections reported by Purkait et al. [60] for process (9.5) are close to the results from the CB1-4B method and the experimental data from Fig. 11. Nevertheless, this needs to be reassessed by taking into account the final excited states of the Li^+ ion in process (9.5), since they have been neglected by both Belkić [5] and Purkait et al. [60].

Gayet et al. [100] have also studied process (9.5). They used the CDW-EIS-4B method at impact energies 700–5000 keV (recall that CDW-EIS-4B ≡ CDW-EIS-4B1). Their total cross sections grossly underestimate the experimental data from Fig. 11 by two orders of magnitude. This fact and a similar observation, which we have already made for process (9.2), indicate that the CDW-EIS-4B method is inadequate for double electron capture in heavy particle collisions.

It is also instructive to consider the IPM for reaction (9.2). According to the IPM, the transition amplitude for double electron capture is given as a product of the amplitudes for single electron capture [101–104]. The differential cross section for double electron capture in the IPM version of the CDW method (denoted by CDW-IPM) is the Fourier–Bessel transform:

$$\frac{\mathrm{d}Q_{if}^{(\mathrm{CDW-IPM})}}{\mathrm{d}\Omega} = \left| i v \mu \int_0^\infty \mathrm{d}\rho\, \rho^{1+2iv} \left[a_{if}^{(\mathrm{CDW-3B})}(\rho) \right]^2 J_0(\eta\rho) \right|^2 \left(\frac{a_0^2}{sr} \right). \tag{9.6}$$

Here, $a_{if}^{(\mathrm{CDW-3B})}(\rho)$ is the transition amplitude as a function of ρ in the CDW-3B method [8,18] for single electron capture (2.7). The expression for $a_{if}^{(\mathrm{CDW-3B})}(\rho)$ in the prior form is given by Belkić and Salin [27] as:

$$a_{if}^{(\mathrm{CDW-3B})}(\rho) = \frac{32i}{v} (Z_\mathrm{P} Z_\mathrm{T})^{5/2} N^+(\nu_\mathrm{P}) N^+(\nu_\mathrm{T}) \left[(1 - i\nu_\mathrm{T}) I_0 + i\nu_\mathrm{T} I_1 \right],$$

where $N^+(\nu_\mathrm{K}) = \Gamma(1 - i\nu_\mathrm{K}) \exp(\pi\nu_\mathrm{K}/2)$, $\nu_\mathrm{K} = Z_\mathrm{K}/v$ (K = P, T) and

$$I_0 = \int_0^\infty \mathrm{d}\kappa\, \kappa J_0(\kappa\rho) \frac{A}{C^2} \left(1 - \frac{\omega_1}{\kappa^2 + \gamma^2} \right)^{-1-i\nu_\mathrm{P}} \left(1 - \frac{\omega_2}{\kappa^2 + \delta^2} \right)^{-i\nu_\mathrm{T}},$$

$$I_1 = \int_0^\infty \mathrm{d}\kappa\, \kappa J_0(\kappa\rho) \frac{A + iB}{C^2} \left(1 - \frac{\omega_1}{\kappa^2 + \gamma^2} \right)^{-1-i\nu_\mathrm{P}} \left(1 - \frac{\omega_2}{\kappa^2 + \delta^2} \right)^{-1-i\nu_\mathrm{T}},$$

$$\begin{aligned}
&A = \kappa^2 + \delta^2 - (Z_\mathrm{P} + iv)(Z_\mathrm{P} - i\alpha), \quad B = v(Z_\mathrm{P} - i\alpha), \\
&\gamma = \alpha^2 + Z_\mathrm{P}^2, \quad \alpha = \frac{v}{2} - \frac{E_i - E_f}{v}, \quad \omega_1 = 2v(\alpha + iZ_\mathrm{P}), \\
&\delta = \beta^2 + Z_\mathrm{T}^2, \quad \beta = \frac{v}{2} + \frac{E_i - E_f}{v}, \quad \omega_2 = 2v(\beta + iZ_\mathrm{T}), \\
&C = (\kappa^2 + \gamma^2)(\kappa^2 + \delta^2), \quad \gamma = \delta.
\end{aligned}$$

The total cross sections $Q_{if}^{(\mathrm{CDW-IPM})}$ are computed from (9.6) by standard integration over ρ in the interval $[0, \infty]$. The ensuing results have been reported by Belkić et al. [22]. These latter results are in satisfactory agreement with measurements in the energy range 0.9–7 MeV (not shown in Fig. 10 to avoid clutter, but similar results from CDW-IPM will be displayed in Fig. 12). Additional computations have been performed in the CDW-IPM using the Hylleraas wave function [72] for the final bound state φ_f, and the RHF orbital [105–107] for φ_i, which is expressed in an analytical form as given by Clementi and Roetti [108]. These latter results, denoted by $Q_{if}^{(\mathrm{CDW-IPM)(ii)}}$ have been compared by Belkić et al. [22] with the cross sections $Q_{if}^{(\mathrm{CDW-IPM)(i)}}$ computed by means of the orbital of Hylleraas [72] for both the initial and final bound states. In Ref. [22] it was found that at lower and intermediate energies 100–1000 keV the results for $Q_{if}^{(\mathrm{CDW-IPM)(ii)}}$ are smaller than those for $Q_{if}^{(\mathrm{CDW-IPM)(i)}}$ by a factor $\gamma' \equiv Q_{if}^{(\mathrm{CDW-IPM)(ii)}} \big/ Q_{if}^{(\mathrm{CDW-IPM)(i)}}$ with the numerical values confined to the interval $\gamma' \in [0.90, 0.52]$. Such a pattern is precisely reversed at higher energies from 1 to 7 MeV at which $\gamma' \in [0.90, 1.65]$. The difference between the results $Q_{if}^{(\mathrm{CDW-IPM)(i)}}$ and $Q_{if}^{(\mathrm{CDW-IPM)(ii)}}$ is a well-known consequence of electronic correlations. Radial correlations are abundantly present in the RHF orbital [108], whereas they are ignored in the Hylleraas wave function.[3] The IPM and the related independent event model (IEM) [109] completely ignore the dynamic correlation effects that make double charge exchange fundamentally different from single electron transfer. Nevertheless, both the IPM and IEM can be amended by incorporating static correlations. This has been shown by Crothers and McCarroll [109] who used the IEM within the CDW method (as denoted by CDW-IEM) to study double electron capture in the He^{2+}–$He(1s^2)$ collisions. They included the static electron correlation effects in the target through the wave function of Pluvinage [110,111] with the explicit appearance of the inter-electronic coordinate r_{12}. Deco and Grün [104] used the CDW-IPM with target static correlation effects included by means of the configuration interaction (CI) wave functions (also called linear superposition of configurations).

9.2 Double electron capture into excited states

The prediction of the contributions from excited states requires a convenient description of singly and doubly excited states of a helium-like atomic system. One possibility is to describe the final state $\varphi_f(\boldsymbol{s}_1, \boldsymbol{s}_2)$ by means of the CI wave function. For these CI functions, the procedure to calculate the bound-free form factors as the matrix elements in the CDW-4B method has previously been devised by Belkić and Mančev [7] in a general manner, which is applicable to both the ground and excited states of helium-like atoms or ions. This can be done by employing a basis set of mono-electronic functions such as Slater type orbitals (STO) or hydrogen-like orbitals with a nuclear charge Z_P [112,113]. Such functions are particularly convenient for describing singly or doubly excited states. When the final state is auto-ionizing, only the bound

[3] In the Hylleraas wave function of helium-like atoms, merely the Slater screening is taken into account by which the nuclear charge Z_T is replaced with $Z_\mathrm{T} - 5/16 = Z_\mathrm{T} - 0.3125$.

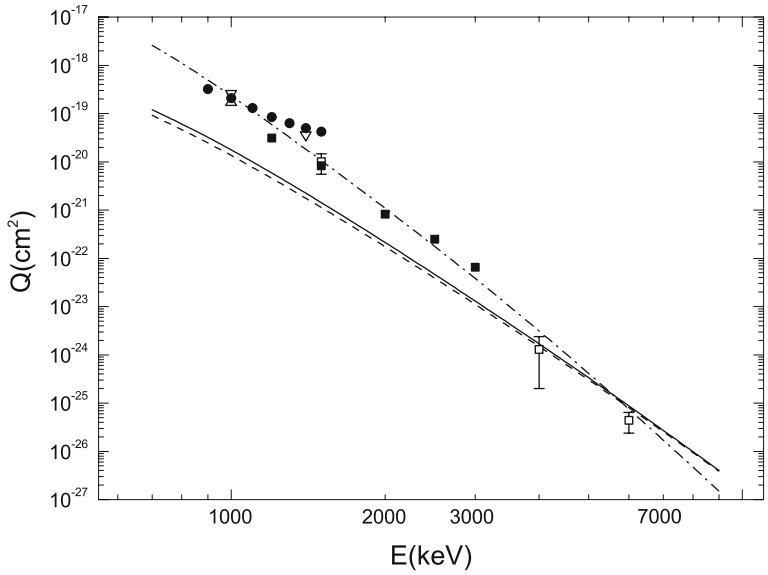

Fig. 12 Total cross sections Q as a function of the incident energy E for process $He^{2+} + He(1s^2) \rightarrow He(\Sigma) + He^{2+}$. Theory: *singly-chained curve* (CDW-IPM method [121] including the sum of the ground and all excited final states), *dashed curve* (CDW-4B method [113] including the final ground state alone), and *full curve* (CDW-4B method [113] including the sum of the ground and all excited final states). Experiment: *filled square* [85], *open down triangle* [88], *open up triangle* [89], *open square* [90] and *filled circles* [91]

components of $\varphi_f(\boldsymbol{s}_1, \boldsymbol{s}_2)$ are kept throughout, since its decay occurs much after the collision has been completed. The use of these CI wave functions [112] within the said procedure of Belkić and Mančev [7] regarding bound-free form factors facilitates the calculation of the matrix elements in the transition amplitude for double electron capture into excited states [113]. These latter calculations were restricted to the singly excited states $(1snl)$ with $n \leq 3$ and $l \leq n-1$ and doubly excited states $(2l2l')$ with $l, l' \leq 1$.

Although other singly excited states should be included, this procedure could provide an initial indication about the contribution from excited states relative to the ground state. The scattering integrals that appear in the calculation with wave functions for excited state are of the type considered by Nordsieck [114]. The explicit methods that bypass the cumbersome and implicit differentiation for calculating the most general cases of these scalar and vectorial bound-free form factors, have been developed by Belkić [115–120] in both parabolic and spherical coordinates.

Total cross sections in the CDW-4B method for double electron capture from He by He^{2+} including several excited states have been reported in Ref. [113]. These results are based upon the wave function of Löwdin [75] for helium in the entrance channel and the CI wave function [112] for the final state in the exit channel. From the outset, capture into excited states is not expected to play a significant role in process (9.2), because of the dominance of the ground-to-ground state transition which is resonant. The explicit computations from Ref. [113] confirm this expectation, such that the sum from all the

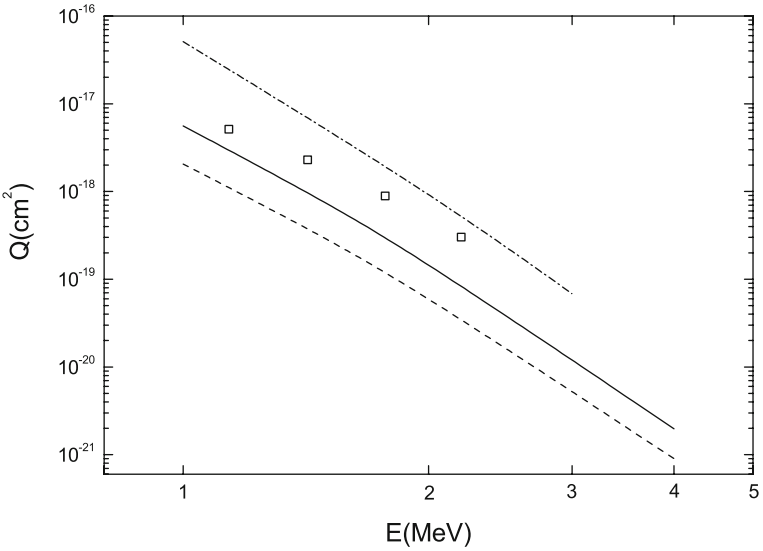

Fig. 13 Total cross sections Q as a function of the incident energy E for process $Li^{3+} + He(1s^2) \rightarrow Li^{+}(\Sigma) + He^{2+}$. Theory: *singly-chained curve* (CDW-IPM method [121] including the sum of the ground and all excited final states), *dashed curve* (CDW-4B method [113] including the final ground state alone) and *full curve* (CDW-4B method [113] including the sum of the ground and all excited final states). Experiment: *open square* [99]

considered final bound states of helium is very close to the full curve in Fig. 10 from the CDW-4B method for the ground-to-ground state transition alone considered by Belkić [21]. This is evidenced directly in Fig. 12. Here, e.g. at the incident energies 1, 2 and 5 MeV the total cross sections from the ground-to-ground state transition (and the sum of this latter contribution with the corresponding yield from the excited states, written in the parentheses) are: $1.48 \times 10^{-20}\text{cm}^2$ $(1.97 \times 10^{-20}\text{cm}^2)$, $1.89 \times 10^{-22}\text{cm}^2$ $(2.33 \times 10^{-22}\text{cm}^2)$ and $3.25 \times 10^{-25}\text{cm}^2$ $(3.60 \times 10^{-25}\text{cm}^2)$, respectively. Moreover, the cross sections due to doubly excited state are smaller than those for singly excited ones, especially at high impact energies [113].

The CDW-4B method used in Ref. [113] has also been applied to double electron capture in the Li^{3+}–He and B^{5+}–He collisions. Here, it is anticipated that the contributions from the excited states are important, as confirmed in Figs. 13 and 14. This occurs because the ground-to-ground transitions for the Li^{3+}–He and B^{5+}–He double charge exchange are non-resonant and, therefore, excited states could yield a sizeable contribution. At smaller impact energies, the main contribution to the total cross section originates from singly excited states, while the ground state $(1s^2)\,^1S$ provides about 40% of the total cross section. In all the cases under consideration, the difference between the cross sections for the ground state and singly excited states diminishes with increased impact energy. It is clear that the ground state contribution dominates at very high impact energies.

The cross sections for formation of doubly excited states are one order of magnitude smaller than the cross sections for singly excited states in the investigated energy

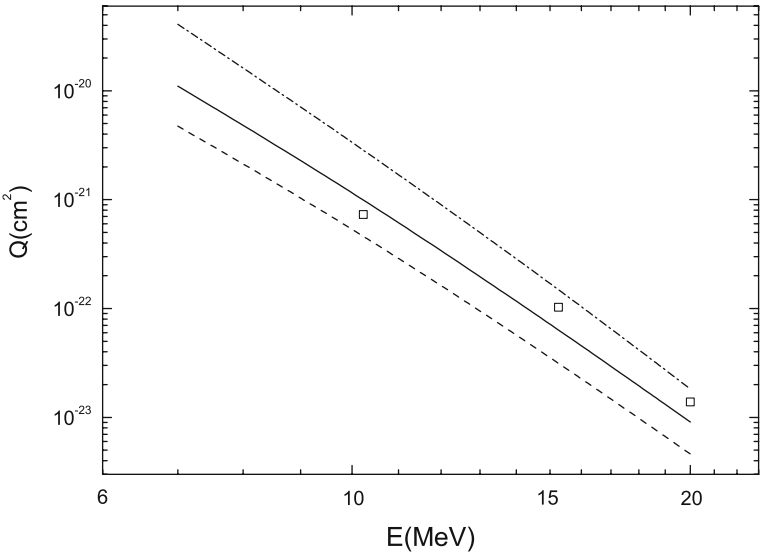

Fig. 14 Total cross sections Q as a function of the incident energy E for process $B^{5+} + He(1s^2) \rightarrow B^{3+}(\Sigma) + He^{2+}$. Theory: *singly-chained curve* (CDW-IPM method [121] including the sum of the ground and all excited final states), *dashed curve* (CDW-4B method [113] including the final ground state alone) and *full curve* (CDW-4B method [113] including the sum of the ground and all excited final states). Experiment: *open square* [122]

range. Furthermore, for the Li^{3+}–He and B^{5+}–He collisions, the contributions from the states $(1s3s)\,^1S$ and $(1s3p)\,^1P$ become of the order of or even significantly larger than the ones from the states $(1s2s)\,^1S$ and $(1s2p)\,^1P$ in the investigated energy region [113]. The results from the CDW-IPM [121] are also shown in Figs. 13 and 14. These results correspond to double electron capture into all final states of the $(Z_P; e_1, e_2)_f$ system, and they are seen to overestimate the experimental data.

The main goal of this subsection is to assess the contribution of excited states from the $(Z_P; e_1, e_2)_f$ system in the exit channel of process (2.1). It is found that these latter contributions can be important, provided that the studied transitions are non-resonant when the target is in the ground state, as usual. Moreover, the inclusion of excited states into the computation can noticeably improve agreement between the CDW-4B method and experimental data, as in the case of the Li^{3+}–He and B^{5+}–He collisions [121] (although in the former case the results from the CDW-4B method still lie considerably below the measured data, as seen in Fig. 13). However, this is definitely not the case for the He^{2+}–He collision [121], since the ground-to-ground state transition in process (9.2) is dominant due to resonance. Note that for formation of H^- in the H^+–He double charge exchange [7,76], there are no excited states in the exit channel. Hence, it can be concluded that the CDW-4B1 method provides relatively reliable predictions for double electron capture at intermediate and high impact energies for the H^+–He, Li^{3+}–He and the B^{5+}–He collisions, but not for the He^{2+}–He collision, for which an approximate version of the CDW-4B2 method yields good agreement with experiments (see Fig. 10).

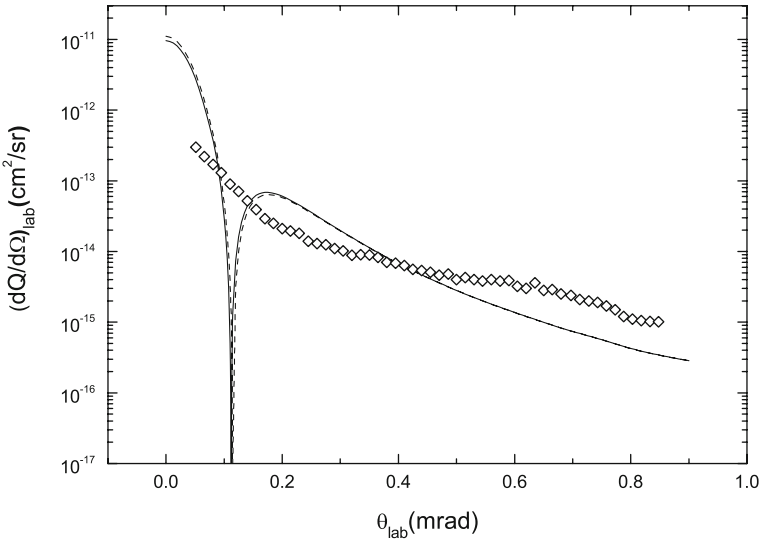

Fig. 15 Differential cross sections $dQ/d\Omega$ as a function of the scattering angle θ at the incident energy $E = 1.5$ MeV for process (9.2). Theory (no convolution): *dashed curve* (CB1-4B method without perturbation O_i [22,69,70]) and *full curve* (CB1-4B method with perturbation O_i [22,70]). Experiment: *open diamond* [85]

It should be noted that the CDW-4B method can also be used with multi-parameter highly correlated wave functions, such as those from Refs. [123–126] that include a number of the CI terms ranging from 12 to 108. These latter orbitals are capable of including most of the radial and angular correlations, despite the fact that such functions do not explicitly contain the inter-electronic coordinate r_{12}. The wave functions from Refs. [125] and [126] have been extensively used by Belkić [127,128] for single electron detachment from $H^-(1s^2)$ by impact of H^+ studied by using the MCB-4B method.

In order to illustrate the validity of the presented distorted wave approximations, angular distributions $dQ/d\Omega$ should also be reviewed. To this end, we analyze the differential cross sections for double electron capture in collisions between the He^{2+} ions and He atoms for reaction (9.2) at $E = 1.5$ MeV. Recall that for this latter symmetric and resonant process, there is no post–prior discrepancy. The results for $dQ/d\Omega$ from the CB1-4B method with and without the initial state perturbation O_i given by (9.3) are displayed on Fig. 15. These two sets of differential cross sections from the CB1-4B method computed using the initial and final helium wave functions of Hylleraas [72] are very close to each other.

As expected, this is in accordance with the similar situation already encountered in Fig. 5 regarding the total cross sections for process (9.2) treated in the CB1-4B method. Thus the corrective perturbation O_i can be ignored for both $dQ/d\Omega$ and Q. It is seen in Fig. 15, that the CB1-4B method exhibits an unphysical and experimentally unobserved dip at $\theta_{lab} \simeq 0.112$ mrad. This extremely sharp dip is due to a strong cancellation of the opposite contributions coming from the repulsive $(2Z_T/R)$ and the

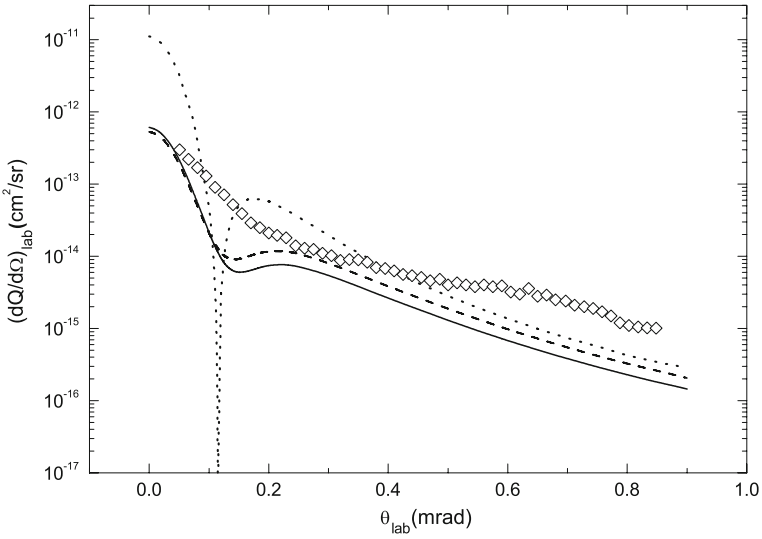

Fig. 16 Differential cross sections $\mathrm{d}Q/\mathrm{d}\Omega$ as a function of the scattering angle θ at the incident energy $E = 1.5$ MeV for process (9.2). Theory (no convolution): *dotted curve* (CB1-4B method [69,70]), *dashed curve* (BCIS-4B method [5]) and *full curve* (BDW-4B method [21,22]). Experiment: *open diamond* [85]

attractive $(-Z_\mathrm{T}/x_1 - Z_\mathrm{T}/x_2)$ potentials in (8.3). In a narrow cone near the forward direction $\theta_\mathrm{lab} \simeq 0$ mrad, the differential cross sections in the CB1-4B method markedly overestimate the experimental findings. On the other hand, as seen in Fig. 15 the CB1-4B method underestimates the experimental data at larger scattering angles.

The differential cross sections obtained using the BDW-4B method are shown in Fig. 16, where a comparison is made with the BCIS-4B and CB1-4B methods, as well as with the experimental data of Schuch et al. [85]. The CB1-4B, BDW-4B and BCIS-4B methods exhibit the proper asymptotic behaviors at large inter-aggregate separations in both the entrance and the exit channels. However, unlike the CB1-4B method, the BDW-4B and BCIS-4B methods take full account of the Coulomb continuum intermediate states of both electrons in one channel. Hence, by comparing these two theories with the CB1-4B method, one could learn about the relative importance of the intermediate electronic ionization continua. As seen in Fig. 16, the BCIS-4B method provides a substantial improvement over the CB1-4B method. First, in the BCIS-4B method, the dip in the angular distribution disappears, and near the dip region the angular distribution exhibits only a minimum at $\theta_\mathrm{lab} \simeq 0.121$ mrad, followed by a neighboring broader maximum (the Thomas peak), despite the fact that the same perturbation potential is used as in the CB1-4B method. The behavior of the angular distribution obtained in the BDW-4B method is altogether quite similar to that in the BCIS-4B method.

It should be recalled that the BDW-4B and BCIS-4B methods differ only in the perturbation potentials, such that the former contains the two gradient operators, whereas the latter uses the scalar (Coulomb) potentials. As can be seen from Fig. 16, the overall agreement of the BDW-4B and BCIS-4B methods with the experimental data can be

considered as fairly good. Nevertheless, at larger scattering angles, despite the proper inclusion of the Rutherford scattering, both the BDW-4B and BCIS-4B methods yield differential cross sections that are considerably lower than the corresponding experimental data [85]. Note that the measured findings relate to double electron capture into all the states of He, whereas the considered theoretical methods include only the ground-to-ground state transition ($1s^2 \rightarrow 1s^2$). The main purpose of Fig. 16 is to demonstrate the influence of electronic intermediate ionization continua to the differential cross sections by direct comparisons among the results of the analyzed four-body methods. None of the theoretical results displayed in Fig. 16 were folded with the experimental resolution function. Further, using (9.6), Belkić et al. [22] also computed differential cross sections by means of the CDW-IPM for reaction (9.2). Their results in the CDW-IPM are in good agreement with the experimental data at small and intermediate scattering angles (not shown in Fig. 16 to avoid clutter). At larger values of θ, the CDW-IPM underestimates the measured data. Unlike the CDW-4B method and the experiment, the CDW-IPM shows some undulations in angular distribution at larger scattering angles [22].

At sufficiently high impact energies, it should be possible to predict three maximae in the differential double capture cross sections. These maximae result from different higher-order contributions as predicted by Belkić et al. [22]. Applying purely classical arguments, one expects to find the customary Thomas double scattering peak at the angle $\theta_{\rm lab}^{(1)} = (1/M_{\rm P})\sin 60^\circ = (1/M_{\rm P})\sqrt{3}/2 \approx 0.118\,{\rm mrad} = 0.0068^\circ$. This peak corresponds to two consecutive events: (i) one electron is captured through the direct first-order mechanism, and (ii) the other electron is captured through the Thomas double scattering. The next similar structure should occur at the angle $\theta_{\rm lab}^{(2)} = 2\theta_{\rm lab}^{(1)} = (2/M_{\rm P})\sin 60^\circ = (1/M_{\rm P})\sqrt{3} \approx 0.236{\rm mrad} = 0.0136^\circ$. In this case, when both electrons are treated classically, they are supposed to be in the same place at the same time to exhibit the cumulative Thomas double scattering. Each electron first scatters elastically on the projectile through 60° towards its parent nucleus. Subsequent scattering of each electron on the target nucleus is also elastic through the next 60°. The two electrons are then ejected from the target with the velocity of the projectile in the incident beam direction. Then the attractive potential between $Z_{\rm P}$ and $2e$ suffices to bind these three particles together into the $(Z_{\rm P}; 2e)_f$ system. These two Thomas peaks have also been analyzed in Ref. [101] within the IPM version of the CDW-EIS method (as acronymed by CDW-EIS-IPM). Their theoretical results for differential cross sections at 400 MeV clearly show the appearance of the structures at $\theta_{\rm lab}^{(1)}$ and $\theta_{\rm lab}^{(2)}$, associated with the mentioned intermediate double scattering processes.

The third peak can be expected at the angle $\theta_{\rm lab}^{(3)} = (1/M_{\rm P})\sqrt{2}\sin 45^\circ = (1/M_{\rm P}) \approx 0.136\,{\rm mrad} = 0.0078^\circ$, which is situated between $\theta_{\rm lab}^{(1)}$ and $\theta_{\rm lab}^{(2)}$. This time, one electron (say, e_1) is first scattered on the projectile through 45° towards the other electron e_2, thus acquiring velocity $v_1 = v\sqrt{2}$. Then, e_1 collides with e_2 elastically and finds itself deflected through another 45° in the incident beam direction with the velocity $v_1' = v$. The consequence of such an event on e_2 is manifested in the recoil of this second electron with speed $v_2 = v$ through 90° perpendicular to the incident direction. In the final step, e_2 scatters elastically on the target nucleus through another 90° with

$v_2' = v$ in the projectile direction. Then both electrons travel in the incident beam direction and are, therefore, captured by the projectile. This event producing the peak at $\theta_{\rm lab}^{(3)}$ represents a genuine third-order effect. The peak at $\theta_{\rm lab}^{(3)}$ is a pure four-body effect due to dynamic correlations. Since these latter correlations are absent from treatments involving independent particles, the peak at $\theta_{\rm lab}^{(3)}$ has not been obtained by Martínez et al. [101] in the CDW-EIS-IPM. In order to adequately describe these higher-order phenomena, it would probably be the most appropriate to use the CB2-4B and CB3-4B methods. In the case of the CB3-4B method, one would encounter multi-dimensional numerical quadratures that could be optimally computed by the Monte Carlo algorithm VEGAS [129–131], as has been shown by Belkić [1,13,95,96].

New experimental data are required at higher impact energies to provide a check of these theoretically predicted peaks in the angular distributions. In addition to the experimental results at 1.5 MeV that represent the first measurement of differential cross sections for double electron capture in the He^{2+}–He collisions, there are also state-selective differential cross sections for the same process at energies 0.25–0.75 MeV [132,133] obtained by using a powerful and versatile atomic microscope type technique known as cold target recoil ion momentum spectroscopy (COLTRIMS). The same COLTRIMS technique has also been used more recently to measure differential cross sections at impact energies ranging from 0.75 to 1.5 MeV/amu [134]. The COLTRIMS technique offers a unique, albeit indirect, but nevertheless extremely precise way to determine the final state of the projectile, including its scattering angles. Instead of energy losses and scattering angles of the projectile itself, COLTRIMS simultaneously determines the longitudinal and transverse momenta of the recoil ion (He^{2+} in the discussed case). Since there are only two particles in the final state, the momentum change of the projectile must be compensated exactly by the momentum change of the recoil ion, as per the total momentum conservation law. Thus analyzing the longitudinal momentum (in the beam direction) of the recoil ion is equivalent to the customary translational spectroscopy of the projectile. Moreover, the determination of the recoil ion transverse momentum is equivalent to measuring the scattering angle of the projectile. Although the achieved scattering angle resolution is better than $\pm 10^{-2}$ mrad [132,133], no structure from the Thomas type mechanisms has been found in these experiments. This indicates that higher impact energies than those considered by Dörner et al. [132,133] seem to be necessary to detect these Thomas peaks unambiguously in the measurements.

10 Discussion and conclusions

This work gives a thorough and systematic evaluation of the current status and a critical assessment of the leading quantum-mechanical four-body distorted wave methods for double charge exchange in high-energy collisions of multiply charged ions with heliumlike targets. Particular emphasis is placed upon the importance of preserving the proper Coulomb boundary conditions that are of high relevance to both the formal establishment of theory and comparisons with measurements. In practice, it is relatively easy to satisfy the correct Coulomb boundary conditions for the initial and final total scattering wave functions in the entrance and exit channels. To this end, in addi-

tion to the long-range Coulomb distortions of the plane waves for relative motion of two charged heavy aggregates, account should be made for the intermediate ionization continua of the electrons in the entrance and exit channels for the CDW-4B method, or in either the entrance or exit channel for hybrid distorted wave treatments, such as the boundary-corrected continuum intermediate state (BCIS-4B) and Born distorted wave (BDW-4B) methods. Regarding the boundary-corrected first Born (CB1-4B) method, the pure electronic continuum intermediate states are not directly taken into account. Rather, the presence of the electrons is felt here through a screening of the two nuclear charges in the Coulomb wave functions of the relative motion of the heavy scattering aggregates.

Double electron capture from helium by fast heavy nuclei is studied by means of the CB1-4B, CDW-4B, BDW-4B, BCIS-4B and CDW-EIS-4B methods. It is found that unlike the well-documented success of the CB1-3B method for single-electron capture at intermediate and a wide range of high energies (all the way up to the outset of the Thomas double scattering), the CB1-4B method, as the prototype of four-body first-order theories, is satisfactory for double electron capture only at some intermediate energies, but dramatically fails at higher energies. By contrast, as the prototype of four-body second-order theories, the CDW-4B method is successful for the majority of double electron capture processes, thus continuing with the excellent tradition of the corresponding three-body counterpart, which is the CDW-3B method. This is particularly true for two-electron capture from He by H^+ for which it is sufficient to include only the ground-to-ground state transition, due to the absence of the excited states of the H^- ion formed in the exit channel. For the same H^+–He double charge exchange, the cross sections from the CB1-4B method markedly overestimate all the experimental data by 1–3 orders of magnitude at all energies (10–1000 keV). Moreover, using the CDW-4B method for double electron capture in the Z_P–He collisions with $Z_P \geq 3$, it is found that the contribution from excited states can be important compared to that from the corresponding ground states. As such, including excited states into computations can improve the agreement between the CDW-4B method and experimental data.

From the terminological viewpoint within the distorted wave formalism, it is customary to refer to the first/second-order methods as those theories that exclude/include the electronic continuum intermediate states, respectively. On the other hand, any such second-order distorted wave method, may simultaneously be the lowest-order term in a consistent perturbation series expansion of the full transition amplitude. Then by a parallel nomenclature, this lowest-order term of a perturbation development (with or without distorted wave formalism) would be called a first-order approximation to the full transition amplitude. Thus, for example, the CDW-4B method is a second-order method (when viewed from the distorted wave perspective), as it includes the electronic continuum intermediate states. However, the same CDW-4B method is simultaneously the rigorous first-order term in the Dodd–Greider perturbation series. As such, the CDW-4B method is also the first-order approximation to the exact Dodd–Greider expansion. This latter fact should explicitly be indicated (whenever there is a chance for confusion) with a more specific acronym such as CDW-4B1. This is especially helpful whenever a reference should be made to the second term in the Dodd–Greider expansion, in which case the acronym CDW-4B2 is definitely needed.

As to double electron capture in the He^{2+}–$He(1s^2)$ collisions, excited states are expected to play a minor role due to the dominance of the resonant $1s^2$–$1s^2$ transition. The CDW-4B method confirms this anticipation, but does not quantitatively reproduce a part of the available experimental data at impact energies 200–3000 keV that are within the domain of the validity of this theory for the He^{2+}–$He(1s^2)$ collisions. Interestingly, for this symmetric scattering, the CB1-4B method substantially outperforms the CDW-4B method at energies 200–1500 keV. Such a surprising situation might seem to have been ameliorated in the past by using a crude approximation to the Green function from the second-order propagator of a perturbation expansion which, however, is not of the Dodd–Greider type. It is well-known that this latter circumstance could lead to certain serious difficulties.

All ordinary distorted wave perturbation expansions (non-Dodd–Greider), similar to the undistorted Born series, contain disconnected or dangerous diagrams that cause the transition operator to diverge for rearranging collisions. A seemingly improved agreement of the 'augmented' CDW-4B method for the two-electron transfer in the He^{2+}–$He(1s^2)$ collisions should therefore be taken with considerable caution, since the approximate Green function is merely off-shell. Moreover, only two hydrogen-like ground states centered on the projectile and target nucleus were taken into account from the sum over the discrete and continuous parts of the whole spectrum. More systematic work is needed for this particular colliding system, first by treating the on- and off-shell contributions on the same footing, and second by assessing the convergence rate in the spectral representation of the Green function from the second-order term of a chosen perturbation series. Needless to say, it would be important to use the second term in the Dodd–Greider perturbation series to obtain a relatively reasonable estimate of the proper CDW-4B2 method for double charge exchange. Comparing such an estimate to the contribution from the associated CDW-4B1 method would give an invaluable indication about convergence of the Dodd–Greider perturbation series which does not contain any disconnected diagrams.

As to the BCIS-4B and BDW-4B methods, they have been applied to double electron capture in the He^{2+}–He collisions. At moderately high energies (1–3 MeV), good agreement with experiments is found using the BCIS-4B and BDW-4B methods. However, at still higher energies (4 and 6 MeV), the cross sections from the BCIS-4B and BDW-4B methods overestimate the experimental findings (that are the only two measured data points above 3 MeV). Below 1 MeV all the way up to 100 keV, the BCIS-4B and BDW-4B methods underestimate the available experimental data by a factor ranging from 2 to 10. Otherwise, throughout the range 100–7000 keV, the BCIS-4B and BDW-4B methods agree closely with each other. They both exhibit a broad Massey maximum near 175 keV. Such a behavior is opposed to the CDW-4B method which gives the cross sections that continue to rise with decreasing impact energy, as usual, without any sign of the resonance peak. This latter pattern occurs because of an enhanced contribution from the discrete-continuum coupling, which is mediated by the typical $\boldsymbol{\nabla} \cdot \boldsymbol{\nabla}$ potential operator (for each of the two electrons) in the perturbation interaction from the transition amplitude of the CDW-4B method. Here, we have an example of discrete-continuum interference, because one gradient in the perturbation acts on e.g. the initial bound state centered on the target nucleus, whereas the other gradient is applied to the electronic full Coulomb wave centered on the projectile.

The gradient–gradient perturbation describes the same electron being simultaneously bound to the target nucleus, and unbound in the field of the projectile nucleus. Therefore, this coupling of discrete and continuum states via $\nabla \cdot \nabla$ is a typical two-center effect. Once the underlining scalar product is carried out, at least two complex-valued terms are obtained in the transition amplitude T_{if}^{-}. The ensuing terms can have constructive or destructive interference in $|T_{if}^{-}|^2$, depending on the value of the impact energy. Specifically, when the impact energy decreases, constructive interference prevails between the two mentioned parts in $|T_{if}^{-}|^2$ and this causes the cross sections to increase in the CDW-4B method. Also, the Coulomb normalization constant for the full electronic continuum intermediate states increases with decreasing energy. These features are common to both the CDW-3B and CDW-4B methods. However, in the CDW-4B method, this constructive interference is further enhanced, since there are two gradient–gradient operators for each of the two actively participating electrons.

The CDW-EIS-4B method, as another hybrid method, was also applied to double capture from helium by alpha particles at impact energies ranging from 0.1 to 6 MeV. This method combines the CDW-4B method for the exit channel with the symmetric eikonal (SE-4B) method in the entrance channel. Unexpectedly, at energies 0.1–3 MeV, the CDW-EIS-4B method fails much more severely than the CDW-4B method for the same collision. Specifically, at energies 0.1–3 MeV the cross sections from the CDW-EIS-4B method underestimate all the experimental data by a factor ranging from 10 to 1000. Only at the two highest energies (4 and 6 MeV), the curve from the CDW-EIS-4B method passes through the estimated error bar limits of the measured cross sections. This breakdown of the CDW-EIS-4B method at energies 0.1–3 MeV is very surprising, especially given the success of the corresponding CDW-EIS-3B method for single electron capture at a wide range of intermediate and high energies. As an attempt to rescue this unsatisfactory situation, the 'augmented' CDW-EIS-4B method has been used in the past by including approximately a second-order term in a non-Dodd–Greider perturbation expansion, in precisely the same manner as done in the discussed 'augmented' CDW-4B method. However, this has not met with success at all and, therefore, further studies are needed to clarify the hidden drawbacks of the CDW-EIS-4B method for double electron capture. Such studies are needed in view of the similar inadequacy of the CDW-EIS-4B method for double electron capture in the Li^{3+}–He collisions. Crucially, no similar inadequacies are present in the BDW-4B and BCIS-4B methods.

Further, we conclude that for double charge exchange, the presented four-body methods are weakly dependent upon the choice of bound state wave functions. By implication, static correlations of two electrons bound to the target do not play a significant role in double electron capture.

The present work is also concerned with analyzing the role of continuum intermediate states of the electrons in the field of nuclei in the entrance and exit channels. The net effect of these latter states is observed to be striking, as illustrated in the case of symmetric resonant double-charge transfer in the He^{2+}–He collisions at high energies. For example, during comparisons of theory with measurements at high energies, it was found that the BCIS-4B method markedly improves (by 2 orders of magnitude) the predictions of the CB1-4B method. This startling effect occurs because the

BCIS-4B method describes the motion of two electrons in the field of the projectile by two full Coulomb waves that are in the CB1-4B method approximated by their asymptotes (logarithmic phases) in terms of the variable $\boldsymbol{R}$, which is vector of the distance R between the two heavy scattering aggregates. Hence, a comparative analysis of the BCIS-4B and CB1-4B methods reveals the critical importance of the electronic continuum intermediate states for double charge exchange. While the CB1-3B and BCIS-3B methods for single electron transfer collisions give cross sections that are similar at all energies prior to the outset of the Thomas region, the corresponding CB1-4B and BCIS-4B methods depart from each other progressively more severely with increasing impact energies. This indicates that continuum intermediate states are much more important for four- than for three-body fast collisions.

Yet another instructive insight could be gained by examining the sensitivity of continuum intermediates states to the explicit form of the distortion of the wave function within e.g., the initial scattering state. The first invaluable hint is provided already by the discussed comparison between the CDW-4B and CDW-EIS-4B methods. Recall that the latter is a further approximation of the former. The additional approximation is in the replacement of the two electronic full Coulomb waves in the entrance channel by their logarithmic phase factors that are valid at asymptotically large distances. Everything else remains the same in the T-matrix elements from the CDW-4B and CDW-EIS-4B methods. An analogous replacement in the CDW-EIS-3B method gives total cross sections that typically bend down towards the experimental data as opposed to departing from them, as is the case with the CDW-3B method. The resulting agreement with experiments created enthusiasm about the CDW-EIS-3B method, although no rationale for the success has ever been reported. It is indeed counter-intuitive that an approximation to a given method works better than the exact version of that method itself (CDW-EIS-3B versus CDW-3B in the case under discussion). This remark cannot be countered by the argument that the CDW-EIS-3B method is derivable with no reference to the CDW-3B method. Namely, irrespective of the derivation, the final expression for the post transition amplitude in the CDW-EIS-3B method is immediately identified as the eikonal approximation of the corresponding exact CDW-3B method in which the full Coulomb wave in the entrance channel is replaced by its logarithmic phase asymptote.

An important question to ask here is: does the improvement of the CDW-EIS-3B over CDW-3B method occur at the energies within the assessed validity domain of high-energy methods? Both the CDW-3B and CDW-EIS-3B methods are high-energy approximations as the lowest (first) orders in the Dodd–Greider perturbation expansion of the complete transition amplitude. This implies that they should be valid at impact velocities v exceeding (typically by several times) the classical orbital velocity v_0 of the electrons from the target state from which double capture takes place. At these latter impact velocities ($v \gg v_0$) from the domain of the joint validity, excellent agreement exists between the CDW-3B and CDW-EIS-3B methods that, in turn, compare favorably with measurements. However, improvement of the CDW-EIS-3B method over the CDW-3B method occurs outside the expected validity domain of both methods, i.e., at those values of v that are close and smaller than v_0. As such, the answer to the raised question is in the negative. In other words, the improvement of the CDW-EIS-3B over CDW-3B method comes at energies at which it is not theoret-

ically expected from the applicability criterion for the lowest-orders of perturbation series expansions. Technically, the reduction of large cross sections from the CDW-3B method in the region below its domain of applicability is achieved by simplifying this theory via eikonalization which yields the CDW-EIS-3B method. The eikonalization succeeds in weakening the intensity of bound-continuum coupling. This is possible by an admixture of destructive interference caused by approximating the full Coulomb wave by its asymptotic phase in the entrance channel. Such an outcome is plausible, since interference in $|T_{if}|^2$ is very sensitive to any change of phases in all the complex-valued constituents of the T-matrix element. Consequently, constructive interference from the CDW-3B method at lower energies can be mitigated or even converted into destructive interference when Coulomb waves are replaced by their asymptotes. And this is what happens in the CDW-EIS-3B method. Added to this destructive interference is the absence of the normalization constant in the Coulomb wave function in the eikonal initial state from the CDW-EIS-3B method. This Coulomb normalization increases with decreasing incident velocity.

In order not to view this switching (from constructive to destructive interference) as fortuitous and limited only to one active electron, it would be necessary that a similar phenomenon also occurs within eikonalization of electronic full Coulomb waves for two or more active electrons. This is indeed the case with the CDW-EIS-4B method for two-electron capture. The only problem is that this time the benefit of the CDW-EIS-3B method from destructive interference is not repeated at all by the CDW-EIS-4B method. Quite the contrary, the replacement of two electronic full Coulomb waves by the corresponding double phase factor in the entrance channel yields a markedly exaggerated destructive interference. Astoundingly, the CDW-EIS-4B method gives cross sections that grossly underestimate experimental data as well as the results from CDW-4B method by 1–3 orders of magnitude at the energies from the expected theoretical domain of validity (0.1–3 MeV). This effectively pushes the lower limit of the applicability domain of the CDW-EIS-4B method to quite high energies ($E \geq 4$ MeV). On the other hand, the CDW-EIS-4B method is not adequate at energies where the Thomas double scattering becomes important, because the eikonalization of Coulomb waves destroys the proper velocity dependence for spherically non-symmetric states. As such, the domain of applicability of the CDW-EIS-4B method is restricted to a very narrow interval indeed (nearly void of experimental data) which is embedded in the high energy region. In practice, this excludes the CDW-EIS-4B method from the list of useful approximations for double electron capture.

Hence, there are no systematics in improving the CDW by the CDW-EIS model when passing from single- to double-electron capture. Rather, quite the contrary happens. This indicates that the CDW-EIS method works for single capture by serendipity, but fails as soon as the physics and testings become more stringent, which is the case for double capture. This was bound to happen, since the CDW-EIS method is merely an eikonal approximation to the CDW method, as stated. Therefore, rather than resorting to comparisons with experiments, the genuine quality of this eikonalization must first and foremost be judged by the departure of the CDW-EIS from the CDW method within their joint domain of validity as high-energy theories. Experiments on single capture happened to favor the CDW-EIS over the CDW method at energies where neither method was expected to be adequate. However, if the course of the events had

been otherwise in the past, with testings of the CDW-EIS method against the experiment being performed first on double capture, this eikonal model would be considered as utterly inadequate. At present, regarding capture processes alone, all we can say is that the CDW-EIS method is limited exclusively to single capture. Multiple capture is expected to be even more devastating for the CDW-EIS method than double capture, since probably with every additional electron becoming active, another higher order in the corresponding perturbation expansion would be necessary for a barely qualitative description, but on the expense of rendering the computations prohibitively impractical. This is an extrapolation of the current experience with a second-order CDW-EIS method which can hardly follow the shape of the line drawn through experimental data on double capture let alone quantitatively reproduce the measured cross sections. Whether these severe drawbacks and limitations also extend to double and multiple ionization remains to be seen. Thus far, the CDW-4B and CDW-EIS-4B methods have not been applied to double ionization in collisions of nuclei with helium-like atomic systems. Both the CDW-3B and CDW-EIS-3B methods are excellent for single ionization of hydrogen-like and multi-electron atomic targets by fast nuclei. For highly charged projectiles, it has been demonstrated in the literature that the CDW-3B method outperforms the CDW-EIS-3B approximation.

Also illustrative is to juxtapose the BDW-4B and CDW-EIS-4B methods. This is interesting because the BDW-4B method differs from the CDW-EIS-4B method only in the inter-particle variables from the Coulomb logarithmic phase factors in the entrance channel. This variable is the inter-aggregate separation $\boldsymbol{R}$ in the BDW-4B method. In the CDW-EIS-4B method, a pair of two different variables ($\boldsymbol{s}_1$ and $\boldsymbol{s}_2$) appears as the distances of the two electrons from the projectile nucleus. This leads to two Coulomb logarithmic phase factors for the motion of two electrons in the field of the projectile nucleus. As stated, two such phases are the asymptotic forms of the corresponding full Coulomb wave functions for the electrons in the projectile-nucleus field. In the asymptotic region with large distances among all the particles, the product of the two electronic Coulomb phases in the CDW-EIS-4B method coincides with the corresponding logarithmic factor from the BDW-4B method. Such a high degree of similarity between these two methods also exists in the corresponding versions for one-electron transitions, such that the CDW-EIS-3B and BDW-3B methods give cross sections that are quite close to each other. However, this is not the case any longer for double capture, since the CDW-EIS-4B method underestimates the BDW-4B method by 1–2 orders of magnitude at all energies (0.1–6 MeV).

One wonders why the passage from the CDW-EIS-3B to CDW-EIS-4B method is so troublesome, as opposed to the extension of the BDW-3B to BDW-4B method? The answer is that the BDW-4B and CDW-EIS-4B methods have very different phase interference patterns away from large inter-particle separations. In the CDW-EIS-4B method, the Coulomb logarithmic phases for the eikonal initial state are always of a purely electronic origin (at all distances, finite and infinite), as is the discrete-continuum coupling via $\boldsymbol{\nabla} \cdot \boldsymbol{\nabla}$ in the perturbation potential, which causes the transition in the T-matrix element. For each of the two electrons, this latter two-center coupling is such that one of the gradient operators in the scalar product $\boldsymbol{\nabla} \cdot \boldsymbol{\nabla}$ acts on the final bound state in the field of the projectile nucleus, whereas the other applies to the electronic full Coulomb wave function centered on the target nucleus. As discussed, at finite

distances the two electronic phase factors in the entrance channel introduce a strong destructive interference into the discrete-continuum coupling, thus yielding an enormous reduction of the ensuing cross sections in the CDW-EIS-4B versus CDW-4B method. This is one of the origins of the worsened agreement of the CDW-EIS-4B method with experiments. The other origin is the absence of the normalization constants of the two Coulomb wave functions, as a consequence of their eikonalization. In contradistinction, the Coulomb phases in the BDW-4B method are in terms of the inter-aggregate distance R. As such, they do not interfere significantly (at finite separations) with the electronic discrete-continuum coupling mediated by the same $\nabla \cdot \nabla$ potential operator which is common to both the BDW-4B and CDW-EIS-4B methods. More precisely, unlike the electronic logarithmic factors from the CDW-EIS-4B method, the scattering integrals involving the $\boldsymbol{R}$-dependent phases from T_{if} in the BDW-4B method are reduced to a folding- or convolution-type integral. As a result, even if destructive interference effects from the $\boldsymbol{R}$-dependent eikonal phases are present, they are effectively damped by this additional integration (folding). Recall that, by definition, every integral acts as a smoothing operator, which de facto averages over sharp phase-sensitive oscillations/undulations of the integrand. Additionally, the discrepancy between the total cross sections from the CDW-EIS-4B and BDW-4B methods increases with decreasing impact energy, attaining the largest values in the region of the Massey resonance peak. This is another independent confirmation of the critical relevance of phase interference effects that are radically different in these two methods. It should be recalled that the prominent role in any resonance phenomena is played by phases of functions whose interference can greatly influence the heights of resonant peaks. To recapitulate, as far as one is dealing with the continuum intermediate states, the common conclusion which emerges from the comparative analysis of the CDW-4B, BDW-4B and CDW-EIS-4B method is that the replacement of the full purely electronic Coulomb waves by their eikonal phases in the CDW-EIS-4B method is entirely unjustified.

We can conclude that at least some of the presently analyzed quantum mechanical boundary-corrected four-body methods are able to provide adequate results for single as well as double electron transitions at intermediate and high energies. Interest in these methods remains steady, and further progress is expected in their extensions to pure five-body scattering problems without resorting to the customary frozen-core approximation, in order to adequately describe the existing coincidence experiments with three active electrons.

Acknowledgments This work was supported by the Swedish Cancer Society Research Fund and King Gustav the Fifth's Jubilee Foundation.

References

1. Dž. Belkić, *Principles of quantum scattering theory* (Institute of Physics Publishing, Bristol, 2004)
2. Dž. Belkić, *Quantum theory of high-energy ion-atom collisions* (Taylor and Francis, London, 2008)
3. Dž. Belkić, I. Mančev, J. Hanssen, Rev. Mod. Phys. **80**, 249–314 (2008)
4. Dž. Belkić, Adv. Quantum Chem. **56**, 251–321 (2009)
5. Dž. Belkić, Phys. Rev. A **47**, 3824–3844 (1993)
6. A.E. Martínez, R.D. Rivarola, R. Gayet, J. Hanssen, Phys. Scr. T **80**, 124–127 (1999)

7. Dž. Belkić, I. Mančev, Phys. Scr. **45**, 35–42 (1992)
8. Dž. Belkić, R. Gayet, A. Salin, Phys. Rep. **56**, 279–369 (1979)
9. B.H. Bransden, D.P. Dewangan, Adv. Atomic Mol. Opt. Phys. **25**, 343–374 (1988)
10. B.H. Bransden, M.R.C. McDowell, *Charge exchange and the theory of ion-atom collisions.* The international series of monographs in physics (Clarendon, Oxford, 1992)
11. D.S.F. Crothers, L.J. Dubé, Adv. Atomic Mol. Opt. Phys. **30**, 287–337 (1993)
12. D.P. Dewangan, J. Eichler, Phys. Rep. **247**, 59–219 (1994)
13. Dž. Belkić, J. Comput. Meth. Sci. Eng. **1**, 1–74 (2001)
14. B.H. Bransden, C.J. Joachain, *Physics of atoms and molecules*, 2nd edn. (Prentice Hall, New York, 2003)
15. D.S.F. Crothers, J.F. McCann, J. Phys. B **16**, 3229–3242 (1983)
16. P.D. Fainstein, V.H. Ponce, R.D. Rivarola, J. Phys. B **24**, 3091–3119 (1991)
17. N. Stolterfoht, R. DuBois, R.D. Rivarola, *Electron emission in heavy ion-atom collisions* (Springer, Berlin, 1997)
18. I.M. Cheshire, Proc. Phys. Soc. **84**, 89–98 (1964)
19. Dž. Belkić, J. Phys. B **11**, 3529–3552 (1978)
20. D.S.F. Crothers, J. Phys. B **15**, 2061–2074 (1982)
21. Dž. Belkić, Nucl. Inst. Meth. Phys. Res. B **86**, 62–81 (1994)
22. Dž. Belkić, I. Mančev, M. Mudrinić, Phys. Rev. A **49**, 3646–3658 (1994)
23. L.R. Dodd, K.R. Greider, Phys. Rev. **146**, 675–686 (1966)
24. J.F. McCann, J. Phys. B **25**, 449–461 (1992)
25. R.T. Pedlow, S.F.C. O'Rourke, D.S.F. Crothers, Phys. Rev. A **72**, 062719 (2005)
26. Dž. Belkić, A. Salin, J. Phys. B **9**, L397–L402 (1976)
27. Dž. Belkić, A. Salin, J. Phys. B **11**, 3905–3911 (1978)
28. R.D. Rivarola, R.D. Piacentini, A. Salin, Dž. Belkić, J. Phys. B **13**, 2601–2609 (1980)
29. Dž. Belkić, Phys. Rev. A **37**, 55–67 (1988)
30. M. Abramowitz, I. Stegun, *Handbook of mathematical functions* (Dover, New York, 1956)
31. W. Press, S. Teukolsky, W. Vetterling, B. Flannery, *Numerical recipes in Fortran 77: the art of scientific computing* (Cambridge University Press, Cambridge, 1992)
32. L.H. Thomas, Proc. R. Soc. Lond. A **114**, 561–576 (1927)
33. A. Salin, J. Phys. B **3**, 937–951 (1970)
34. Dž. Belkić, R. Janev, J. Phys. B **6**, 1020–1027 (1973)
35. Dž. Belkić, R.K. Janev, J. Phys. B **6**, 2613–2617 (1973)
36. Dž. Belkić, R. Gayet, J. Phys. B **10**, 1911–1921 (1977)
37. Dž. Belkić, R. Gayet, J. Phys. B **10**, 1923–1932 (1977)
38. Dž. Belkić, R. McCarroll, J. Phys. B **10**, 1933–1943 (1977)
39. K.E. Banyard, B. Szuster, J. Phys. B **10**, L503–L511 (1977)
40. K.E. Banyard, B. Szuster, Phys. Rev. A **16**, 129–132 (1977)
41. J.C. Moore, K.E. Banyard, J. Phys. B **11**, 1613–1621 (1978)
42. K.E. Banyard, G.W. Shirtcliffe, J. Phys. B **12**, 3247–3256 (1979)
43. G.W. Shirtcliffe, K.E. Banyard, Phys. Rev. A **21**, 1197–1201 (1980)
44. K.E. Banyard, G.W. Shirtcliffe, Phys. Rev. A **22**, 1452–1454 (1980)
45. Dž. Belkić, R. Gayet, A. Salin, Comput. Phys. Commun. **23**, 153–167 (1981)
46. Dž. Belkić, R. Gayet, A. Salin, Comput. Phys. Commun. **30**, 193–205 (1983)
47. Dž. Belkić, R. Gayet, A. Salin, Comput. Phys. Commun. **32**, 385–397 (1984)
48. A. Chetioui, K. Wohrer, J.P. Rozet, A. Joly, C. Stephan, Dž. Belkić, R. Gayet, A. Salin, J. Phys. B **16**, 3993–4003 (1983)
49. S. Andriamonje, J.F. Chemin, J. Routier, B. Saboya, J.N. Scheurer, Dž. Belkić, R. Gayet, A. Salin, J. Physique **46**, 349–353 (1985)
50. Dž. Belkić, Phys. Scr. **43**, 561–571 (1991)
51. Dž. Belkić, R. Gayet, A. Salin, Atomic Data Nucl. Data Tables **51**, 59–150 (1992)
52. S.D. Kunikeev, J. Phys. B **31**, L849–L853 (1998)
53. M.F. Ferreira da Silva, J. Phys. B **36**, 2357–2370 (2003)
54. I. Mančev, J. Phys. B **36**, 93–104 (2003)
55. I. Mančev, V. Mergel, L. Schmidt, J. Phys. B **36**, 2733–2746 (2003)
56. I. Mančev, J. Comput. Meth. Sci. Eng. **5**, 73–89 (2005)
57. I. Mančev, Europhys. Lett. **69**, 200–206 (2005)

58. Dž. Belkić, J. Phys. B **10**, 3491–3510 (1977) [Corrigendum: Dž. Belkić, J. Phys. B **12**, 337 (1979)]
59. M. Purkait, Eur. Phys. J. D **30**, 11–14 (2004)
60. M. Purkait, S. Sounda, A. Dhara, C.R. Mandal, Phys. Rev. A **74**, 042723 (2006)
61. Dž. Belkić, R. Gayet, J. Hanssen, A. Salin, J. Phys. B **19**, 2945–2953 (1986)
62. Dž. Belkić, S. Saini, H.S. Taylor, Z. Phys. D **3**, 59–76 (1986)
63. Dž. Belkić, S. Saini, H.S. Taylor, Phys. Rev. A **36**, 1601–1617 (1987)
64. Dž. Belkić, H.S. Taylor, Phys. Rev. A **35**, 1991–2006 (1987)
65. D.P. Dewangan, J. Eichler, J. Phys. B **19**, 2939–2944 (1986)
66. Dž. Belkić, Phys. Scr. T **28**, 106–111 (1989)
67. T.P. Grozdanov, P.S. Krstić, Phys. Scr. **38**, 32–36 (1988)
68. S. Alston, Phys. Rev. A **41**, 1705–1708 (1990)
69. Dž. Belkić, Phys. Rev. A **47**, 189–200 (1993)
70. Dž. Belkić, J. Phys. B **26**, 497–508 (1993)
71. L. Gulyás, Gy. Szabo, Z. Phys. D **29**, 115–119 (1994)
72. E.A. Hylleraas, Z. Phys. **54**, 347–366 (1929)
73. J. Silverman, O. Platas, F.A. Matsen, J. Chem. Phys. **32**, 1402–1406 (1960)
74. L.C. Green, M.M. Mulder, M.N. Lewis, J.W. Woll Jr., Phys. Rev. **93**, 757–761 (1954)
75. P.-O. Löwdin, Phys. Rev. **90**, 120–125 (1953)
76. Dž. Belkić, I. Mančev, Phys. Scr. **46**, 18–23 (1993)
77. C.D. Lin, Phys. Rev. A **19**, 1510–1516 (1979)
78. V.I. Gerasimenko, J. Exp. Theor. Phys. **14**, 789–791 (1962)
79. V.I. Gerasimenko, Zh. Eksp. Teor. Fiz. **41**, 1104–1106 (1961)
80. U. Schryber, Helv. Phys. Acta **40**, 1023–1051 (1967)
81. L.H. Toburen, M.Y. Nakai, Phys. Rev. **177**, 191–196 (1969)
82. Y.M. Fogel', R.V. Mitin, V.F. Kozlov, N.D. Romashko, J. Exp. Theor. Phys. **8**, 390–398 (1959)
83. Y.M. Fogel', R.V. Mitin, V.F. Kozlov, N.D. Romashko, Zh. Eksp. Teor. Fiz. **35**, 565–573 (1958)
84. J.F. Williams, Phys. Rev. A **150**, 7–10 (1966)
85. R. Schuch, E. Justiniano, H. Vogt, G. Deco, N. Grün, J. Phys. B **24**, L133–L138 (1991)
86. L.I. Pivovar, M.T. Novikov, V.M. Tubaev, J. Exp. Theor. Phys. **15**, 1035–1039 (1962)
87. L.I. Pivovar, M.T. Novikov, V.M. Tubaev, Zh. Eksp. Teor. Fiz. **42**, 1490–1494 (1962)
88. E.W. McDaniel, M.R. Flannery, H.W. Ellis, F.L. Eisele, W. Pope, US Army Missile Research and Development command technical report, No. H, 1, 78 (1977)
89. R.D. DuBois, Phys. Rev. A **36**, 2585–2593 (1987)
90. N.V. Castro Faria, F.L. Freire Jr., A.G. Pinho, Phys. Rev. A **37**, 280–283 (1988)
91. K.H. Berkner, R.V. Pyle, J.W. Stearns, J.C. Warren, Phys. Rev. **166**, 44–46 (1968)
92. V.I. Gerasimenko, L.N. Rosentsveig, J. Exp. Theor. Phys. **4**, 509–512 (1957)
93. V.I. Gerasimenko, L.N. Rosentsveig, Zh. Eksp. Teor. Fiz. **31**, 684–687 (1956)
94. M.S. Gravielle, J.E. Miraglia, Phys. Rev. A **45**, 2965–2973 (1992)
95. Dž. Belkić, Nucl. Instr. Meth. Phys. Res. B **99**, 218–224 (1995)
96. Dž. Belkić, Phys. Scr. **53**, 414–430 (1996)
97. Dž. Belkić, Nucl. Instr. Meth. Phys. Res. B **154**, 220–246 (1999)
98. V. Mergel, R. Dörner, M. Achler, K. Khayyat, S. Lencinas, J. Euler, O. Jagutzki, S. Nüttgens, M. Unverzagt, L. Spielberger, W. Wu, R. Ali, J. Ullrich, H. Cederquist, A. Salin, C. Wood, R.E. Olson, Dž. Belkić, C.L. Cocke, H. Schmidt-Böcking, Phys. Rev. Lett. **79**, 387–390 (1997)
99. M.B. Shah, H.B. Gilbody, J. Phys. B **18**, 899–913 (1985)
100. R. Gayet, J. Hanssen, A. Martínez, R. Rivarola, Comments Atomic Mol. Phys. **30**, 231–248 (1994)
101. A.E. Martínez, R. Gayet, J. Hanssen, R.D. Rivarola, J. Phys. B **27**, L375–L382 (1994)
102. A.E. Martínez, H.F. Busnengo, R. Gayet, J. Hanssen, R.D. Rivarola, Nucl. Instr. Meth. Phys. Res. B **132**, 344–349 (1997)
103. R. Gayet, J. Hanssen, A. Martínez, R. Rivarola, Z. Phys. D **18**, 345–350 (1991)
104. G. Deco, N. Grün, Z. Phys. D **18**, 339–343 (1991)
105. C.C.J. Roothaan, Rev. Mod. Phys. **23**, 69–89 (1951)
106. C.C.J. Roothaan, Rev. Mod. Phys. **32**, 179–185 (1960)
107. S. Huzinaga, Rev. Phys. **122**, 131–138 (1961)
108. E. Clementi, C. Roetti, Atomic Data Nucl. Data Tables **14**, 177–478 (1974)
109. D.S.F. Crothers, R. McCarroll, J. Phys. B **20**, 2835–2842 (1987)
110. P. Pluvinage, Ann. Phys. NY **5**, 145–152 (1950)

111. P. Pluvinage, J. Phys. Radium **12**, 789–792 (1951)
112. H. Bachau, J. Phys. B **17**, 1771–1784 (1984)
113. R. Gayet, J. Hanssen, L. Jacqui, A. Martínez, R. Rivarola, Phys. Scr. **53**, 549–556 (1996)
114. A. Nordsieck, Phys. Rev. **93**, 785–787 (1954)
115. Dž. Belkić, J. Phys. B **14**, 1907–1914 (1981)
116. Dž Belkić, J. Phys. B **16**, 2773–2784 (1983)
117. Dž. Belkić, J. Phys. B **17**, 3629–3636 (1984)
118. Dž. Belkić, V.Y. Lazur, Z. Phys. A **319**, 261–267 (1984)
119. Dž. Belkić, H.S. Taylor, Phys. Scr. **39**, 226–229 (1989)
120. Dž. Belkić, Phys. Scr. **45**, 9–17 (1992)
121. R. Gayet, J. Hanssen, A. Martínez, R. Rivarola, Nucl. Instr. Meth. Phys. Res. B **86**, 158–160 (1994)
122. R. Hippler, S. Datz, P. Miller, P. Pepmiler, P. Dittner, Phys. Rev. A **35**, 585–590 (1987)
123. F.W. Byron Jr., C.J. Joachain, Phys. Rev. Lett. **16**, 1139–1142 (1966)
124. C.J. Joachain, R. Vanderpoorten, Physica **46**, 333–343 (1970)
125. R.J. Tweed, J. Phys. B **5**, 810–819 (1972)
126. C.J. Joachain, M. Terao, Private communication (1991)
127. Dž. Belkić, Nucl. Instr. Meth. Phys. Res. B **124**, 365–376 (1997)
128. Dž. Belkić, J. Phys. B **30**, 1731–1745 (1997)
129. G.P. Lepage, J. Comput. Phys. **27**, 192–203 (1978)
130. S. Kawabata, Comput. Phys. Commun. **41**, 127–153 (1986)
131. S. Kawabata, Comput. Phys. Commun. **41**, 309–326 (1995)
132. R. Dörner, V. Mergel, L. Spielberger, O. Jagutzki, H. Schmidt-Böcking, J. Ullrich, Phys. Rev. A **57**, 312–317 (1998)
133. R. Dörner, V. Mergel, O. Jagutzki, L. Spielberger, J. Ullrich, R. Moshammer, H. Schmidt-Böcking, Phys. Rep. **330**, 95–192 (2000)
134. R. Dörner, Private communication (2005)